

ABSTRACT

Title of Thesis: A NOVEL AIRFLOW CONTROL VALVE
FOR USE IN MEDICAL APPLICATIONS

Kathryn Elizabeth Hitchcock, Master of Science,
2004

Thesis Directed By: Assistant Professor Dimitrios Hristu-Varsakelis
Department of Mechanical Engineering

Rapid improvements in digital technology over the last two decades have led to artificial ventilators that drastically improve physicians' ability to measure and control aspects of their patients' breathing. However, the mechanical systems paired with the new digital controllers have not advanced in parallel with them. As a result, mechanical ventilators do not respond sufficiently fast to changes in operating conditions and can injure patients by allowing the air volume or pressure in their lungs to become too high. This thesis describes a new air flow control valve that can be incorporated in existing ventilators to correct this condition. The valve's low mass and short stroke result in rapid full-range motion with low actuator force and travel. These qualities also make the valve well-suited for use as a flow-change mechanism in instruments that measure airway resistance, including the Airflow Perturbation Device (APD). We describe a series of experiments that verify the valve's performance in both ventilator and APD applications.

A NOVEL AIRFLOW CONTROL VALVE FOR USE IN MEDICAL
APPLICATIONS

by

Kathryn Elizabeth Hitchcock

Thesis submitted to the Faculty of the Graduate School of the
University of Maryland, College Park, in partial fulfillment
of the requirements for the degree of
Master of Science
2004

Advisory Committee:

Assistant Professor Dimitrios Hristu-Varsakelis, Chair
Professor Arthur T. Johnson
Associate Professor Guangming Zhang

© Copyright by
Kathryn Elizabeth Hitchcock
2004

Acknowledgements

The author wishes to acknowledge and thank the following people for contributing to the completion of this thesis:

Dr. Dimitris Hristu-Versekeli for his extremely patient guidance through four years of balancing personal improvement with service to our nation.

Dr. Arthur T. Johnson for inspiring me to bridge the gap between two disciplines; I would have given up one or the other, and always regretted it.

Dr. Guangming Zhang for reminding me that sometimes experienced researchers have materials problems, too.

Mr. Bernie LaFrance, Mr. Howard Grossenbacher, and Mr. Gary Seibel for helping shape an idea into reality.

Mr. Frank Koh for many patient hours of discussion, devil's advocacy, and just plain cheering up.

Dr. Carl Shanholtz for showing me where I could make a difference, and reminding me that if one person lives when he would have died, then blood, sweat, and tears are not too much to pay.

C, M, H, and P who make everything possible.

Table of Contents

Acknowledgements.....	ii
Table of Contents.....	iii
List of Figures.....	iv
Chapter 1: Introduction.....	1
1.1 Background.....	1
1.2 Contribution.....	4
1.3 Outline.....	5
Chapter 2: Literature Review.....	6
2.1 Pulmonary Support.....	6
2.2 The Measurement of Respiratory Resistance.....	10
2.3 The Role of Valve Design.....	15
Chapter 3: A Novel Air Control Device.....	19
3.1 Design.....	19
3.2 Geometry and Sizing.....	25
3.2.1 Selection of Orifice Shape.....	26
3.2.2 Required Airflow Capacity.....	29
3.2.3 Determination of Valve Dimensions.....	32
3.3 Prediction of Flow Performance.....	34
3.3.1 Throttling Characteristics.....	34
3.3.2 Expected Response to Periodic Actuation.....	36
Chapter 4: Experimental Setup and Procedure.....	41
4.1 Equipment and Instrumentation.....	41
4.1.1 Apparatus.....	41
4.1.2 Instrumentation.....	45
4.2 Experiment One: Static Tests.....	46
4.3 Experiment Two: Dynamic Tests.....	47
4.4 Experiment Three: Resistance Measurement.....	48
Chapter 5: Results and Discussion.....	49
Chapter 6: Conclusions.....	59
6.1 Recommendations for Further Study.....	59

List of Figures

Figure 1: Reduction of Achievable Lung Pressure by Unknown Airway Resistance.....	15
Figure 2: Design Concept.....	20
Figure 3: Internal Parts of Prototype Air Flow Control Device.....	21
Figure 4: Diagram and Photograph of Valve and Housing.....	22
Figure 5: Relationship of Perimeter Change and Area Change for Orifice Shapes for a 0.1 cm Reduction in Perimeter	27
Figure 6: The Range of Valve Motion.....	28
Figure 7: Assignment of Variables for Valve Calculations.....	32
Figure 8: Predicted Throttling Performance of the Valve	35
Figure 9: Comparison of Theoretical Valve Performance with Major Valve Types.....	36
Figure 10: Static Testing Rig.....	42
Figure 11: Dynamic Testing Rig.....	43
Figure 12: Apparatus for Resistance Measurement	44
Figure 13: Flowrate as Function of Changing Gap Size.....	49
Figure 14: Actual Performance of Valve.....	51
Figure 15: Step Input to Valve, Closing.....	53
Figure 16: Valve Response to High Frequencies.....	54
Figure 17: Detailed View of Valve Response to High Frequencies.....	56
Figure 18: Comparison of Current and Proposed APD Performance – Inhalation (top) and Exhalation (bottom).....	57

Chapter 1: Introduction

Without the use of mechanical ventilators, the severely ill and injured often could not survive. Although the evolution of microprocessors over the last few decades has drastically improved the performance of these machines, their secondary effects can cause severe and lasting damage to the body. These injuries are attributed to slow action in the airflow control valves within the ventilators, and to the lack of real-time information concerning the patient's respiratory condition on which to base ventilator settings. The ultimate aim of researchers working to improve these life-saving machines is to provide a continuous measurement of respiratory resistance directly to existing ventilator controllers, and to improve the ventilator's mechanical response in order to achieve high-performance feedback control of the breathing process. This thesis describes the design of a new airflow control device that has the potential to advance the state of the art toward that goal.

1.1 Background

Since the 1500's physicians have explored ways in which to provide artificial respiration for those who, due to injury or illness, are unable to breathe for themselves. Since that time, the science of mechanical ventilation has undergone perpetual improvement and has taken on new roles in medical practice. In addition to preventing immediate death, ventilators are used to reduce the physical cost of gas exchange (that is, the amount of metabolic energy expended on this process), relieve

respiratory muscle fatigue, and allow healing of damaged or diseased tissues that are normally burdened by the breathing process.

In early systems this was accomplished by supplying a fixed, low volume of air to the patient at regular intervals, mimicking the perceived action of the lungs were the patient able to breathe for himself. This approach was based on the belief that people lying supine in hospital beds should not experience dramatic changes in their breathing status like those they would undergo if they were actively exercising. Long experience, however, has shown that this simplistic assumption is not accurate. Beginning particularly during the poliomyelitis epidemic in the United States and Canada in 1952, doctors became aware that patients subjected to artificial ventilation over long periods suffered serious tissue damage due to the mechanical stresses caused by the very machines that were keeping them alive [Hubmayr et al., 1990].

In the decades since then, dozens of schemes have been implemented to reduce the stress that ventilators place on the pulmonary tissues, and to encourage ventilator-dependent patients to more rapidly return to a state of normal breathing. None of these are perfect, and the complicated interdependence of the factors that impact their efficacy results in a lack of concrete proof of their value. The problems common to all are so severe that success achieved by a new approach is generally measured in the associated reduction of the mortality rate.

The task of determining how improvements might be made is not a trivial one. Filling and venting the lungs is not a simple matter of moving air volume into and out of a large, predictable space. The lungs and chest wall are flexible and stretch from their neutral position during inhalation, opposing the flow of air, then provide the

driving force for exhalation through elastic recoil. The airways themselves oppose flow in both directions – they are time-varying constrictions that impose some head loss on the fluid, just as pipes do in mechanical systems [Hubmayr et al, 1990]. This resistance is greater during exhalation than inhalation because pleural pressures are greater than airway pressure in the former case and this causes a reduction in cross-sectional area of smaller, softer-walled airways [Johnson, 1991]. The resistance and elastance vary widely between people, and may change rapidly in an individual, particularly during illness that involves the pulmonary system [Tobin, 2001].

It is clear, then, that the health of the airways is vital to good ventilation. Airway resistance measurements, were they more readily available to health care providers, would be of constant and urgent interest since a sudden or consistent change in this parameter is one excellent indicator of respiratory health. Changes can be caused by allergic reactions, the action of drugs (proper or improper), infection, edema, tissue necrosis, and so forth, in addition to even more dire situations such as a buildup of mucous, blood, or vomit in the airway, all of which may have a serious impact on the health and survival probability of the individual [Walls et al., 1997].

Johnson et al. [1974] created a new mechanism for resistance measurement that will make continuous airway resistance measurements available to the physician, significantly improving the ability to diagnose and treat these acute pulmonary problems, as well as replacing current unsatisfactory methods of diagnosing long-term disease. The APD requires no special maneuver from the patient, and has been proven to be immune to the effects of upper-airway flexibility. Since its inception it has been verified through tests on hundreds of subjects, and meanwhile has

undergone a series of improvements in physical setup and data collection, most notably the use of microprocessors rather than the human eye to compute a resistance value. The next step in the development of this instrument is to employ a robust method of causing steady, dependable changes in the airflow, in place of a current device that is prone to mechanical problems.

Medical device design is complicated and costly, but it seems that the solution to the weaknesses of both the current ventilators and the APD is a new air control device that is robust and can operate at high speeds. This thesis describes just such a valve that shows promise in fulfilling the requirements of both machines. It represents a novel approach to airflow control, and is deliberately designed to minimize bulk and required power in order to optimize performance. These qualities also make it compatible with new technologies in smart materials, particularly electroactive polymers, which are capable of replacing the bulky, high-current actuators used today with light, low-power designs.

1.2 Contribution

This goal of this work was to create a novel air control device designed for rapid actuation. This could be used within mechanical ventilators to produce more rapid changes in flow with the intention of limiting the injurious effects of these machines on the lung. The same design could be used to replace an unsatisfactory flow-change mechanism within an existing respiratory resistance instrument called the Airflow Perturbation Device (APD). This device could also be made compatible with emerging smart materials in order to take advantage of their minimal size and

weight. This thesis describes an air flow control device that can transition between fully open and fully shut over the range of pressures and flows required by mechanical ventilators more rapidly than existing designs. It uses a previously unexplored geometry that minimizes the overall size and the mass of moving parts. It requires minimal control-mechanism stroke. We ensured that the valve possesses favorable throttling characteristics, and verified its ability to produce a smooth curve from full flow to zero flow when desired. Finally we demonstrated the use of the valve as the perturbation mechanism for the APD. This should include provisions for adapting the valve to a design that does not fully close, ensuring a failsafe for uninterrupted breathing to the patient.

1.3 Outline

The remainder of this document is organized as follows. In Chapter Two we review of the role of mechanical ventilators in breathing support, the current science of respiratory resistance measurement, and the current state of the art in the air control devices used in such applications. Chapter Three describes the design pursued in this project, as well as the process of exploration and analysis that led to its final form. Chapter Four provides a detailed description of the testing this new device was subjected to. Finally in Chapters Five and Six we present the results of that testing and some conclusions drawn regarding the outcome of this study as opportunities for further work.

Chapter 2: Literature Review

In this chapter, we will examine the current use and limitations of mechanical ventilation in the hospital setting. We will then explain the history of the Airflow Perturbation Device and explore its applications as the next generation of airway resistance instrument. Finally we will consider the role the valves will play in the advancement of these important life-saving techniques.

2.1 Pulmonary Support

Mechanical ventilators are used to provide gas exchange for patients who are not able to breathe adequately on their own and reduce the breathing effort required of those who are ill or injured. Air is forced into the lungs via a semi-rigid tube placed in the trachea in order to ensure that a sudden swelling of the upper airways or incursion of bodily fluid will not close off the path of flow. Existing ventilators incorporate a number of methods for controlling the flowrate of air, either supplying a specified volume of air per breath, or a specified range of pressures. Breath frequency can be independently selected. The ventilator may perform the entire work of respiration regardless of independent lung action, or may allow the patient to participate in breathing to whatever extent he or she is able. Oxygen enrichment from normal atmospheric partial pressures to nearly pure oxygen may be employed [Gomella, 1998; Tobin, 2001].

There are two basic types of ventilator control. One method is to select the overall volume delivered (tidal volume) and allow the machine to determine the

pressure necessary to force in this quantity against the resistance and elastance of the airways. This entails a risk that the machine may select a high pressure in the presence of strong resistance resulting in barotraumas to the lungs. The other method is to specify a goal inspiratory pressure and program the ventilator to end inspiration when it is reached, which decreases the risk of immediate lung damage but does not guarantee that adequate volume will be delivered to keep the patient alive. Research of the last several years shows that ventilator-induced lung damage can occur while using either mode of control, and is not necessarily directly correlated to the maximum pressure or volumes achieved [Tobin, 2001].

The mechanism of injury caused by mechanical ventilators has not been well explained by research to date, so progress in preventing it has come only as a result of trial and error [Whitehead and Slutsky, 2002]. Immediate evidence of damage appears in the form of air in the intrapleural space of the thorax, the mediastinum, the pericardium, or the pulmonary blood vessels. The lungs hemorrhage and may form clots or begin to fill with blood. The damaged lung tissues stiffen with scars and may become impermeable to gases, rendering them useless in respiration (surgical emphysema). The injured portion of the lung inflames the tissues surrounding it, resulting in their increased susceptibility to damage and a subsequent cascading progression of deterioration. Blood thinners and transfusions used to combat the subsequent systemic effects may result in profuse bleeding and infection that worsen the presenting condition [Gawande, 2003; American Thoracic Society et al., 1999]. Lung tissue cannot be repaired by the body, so the impact of this chain of events will leave a life-long mark on the patient and weaken his or her ability to withstand later

disease [Martini, 1998]. This state of affairs is only acceptable to the medical community because the only alternative is death for their patients.

Clearly some combination of pressures and volumes results in trauma to the lung, but low-volume, low-pressure breaths from a mechanical ventilator can, in some patients, produce just as much damage as elevated levels of either parameter [Matthay, 1999]. Progress in identifying contributing factors is slow. Trials must be performed clinically since the complexity of the blood-lung-airway-machine system in most cases renders useful modeling impossible at the current state of technology. Trials of improved techniques, and even comparisons of existing techniques, are most often conducted empirically since the difficulty of obtaining permission to experiment on these patients in the most delicate of conditions makes standardized approaches rare [Esteban et al, 1995].

A recent study by a group of clinical researchers in this field demonstrated how dramatic an impact even minor improvements can have on the current state of medical science in mechanical ventilation. A multi-center, randomized trial was conducted in which one group of patients with ventilator-stiffened lungs was given slightly lower volumes of air in each breath than dictated by traditional medical practice (6 ml/kg of body weight at 30cm of H₂O or less plateau pressure, versus 12 ml/kg of body weight at 50cm per water or less). The study was so successful beyond expectation that it was stopped when less than half of the intended subjects had been enrolled, and the results were hastily published, resulting in an immediate and permanent change in universal practice. This simple innovation resulted in almost a 9% decrease in mortality, and an average of two fewer days per patient spent on

artificial ventilation (with a presumed concomitant decrease in permanent lung damage) [ARDSNetwork, 2000].

One advancement in ventilator technology that has had an undeniably positive impact on all methods of combating tissue damage was the advent of inexpensive, highly flexible microprocessors that can be used to finely tune the air flow delivered to the patient. Complex feedback loops in which the pressure and volume delivered are sensed at the ventilator outlet and used to tailor subsequent breaths to a pre-determined plan for ventilation have replaced the simple “volume in, volume out” approach that formed the backbone of ventilator science well into the 1980’s.

The speed at which these controls can be effected, though, is still limited by the mechanical devices used to alter air flowrate [Ranieri, 1996]. In a simple open-loop scheme in which air is delivered for pre-determined intervals, ventilators now on the market do not transition between zero and full flow and back again in less than 200 ms [Conti, 1997; Aestiva, 2004; Puritan Bennet 2003]. Since a complete inhalation may need to be as short as 250 ms in the smallest patients (breathing frequency 60 breaths per minute, inhalation to exhalation ratio 1:3), the time required for flow change can represent a significant problem [Catlin, 1998]. This sluggishness interferes with the fine tuning provided by the digital controller and may be the greatest contributing factor in ventilator-induced lung injury. Du et al. [2001] estimate that the electronic controller produces 6-40ms of this delay. A fast-acting flow alteration device is needed in order to minimize the remaining fraction.

Valve lag is an undesirable characteristic in any part of the ventilator system, but is particularly troublesome in the inhalation and exhalation valves, that is, those

which are closest to the patient and determine when the machine-controlled portions of the breath begin and end. During weaning or partial support when the patient also exerts breathing effort, a difference in initiation time between person and machine results in the patient performing isometric exertion against a closed flow pathway. This produces the exact strain and fatigue conditions the ventilator is intended to prevent. In its worst form, the patient ceases to inhale before the valve fully opens, the machine senses the cessation of inhalation effort and elects to not supply a breath, and the patient receives little or no air at all (or conversely is unable to exhale a breath); this condition is called patient-ventilator trigger asynchrony [Chao, 1997]. Other problems thus caused include insufflation lag, in which the patient receives a smaller breath than intended due to slow valve action unrecognized by the ventilator, and run-on in which the ventilator continues to inflate the lungs after the end of intended inspiration. This last is particularly alarming in terms of potential tissue damage. In every form, this poor timing tires the patient and can also cause extreme discomfort, such that sedatives must be given in order to restore even breathing – both results are clearly detrimental to the healing process [Yamada 2000]. Proposing a solution to these serious problems is the target of this research.

2.2 The Measurement of Respiratory Resistance

One important step in reducing ventilator-induced lung injury will be the routine measurement of airway resistance. This is currently clinically assessed in cooperating patients using several methods. Spirometry involves having the patient inhale to maximum capacity then exhale the entire volume forcefully through a

pneumotachograph, and repeating the process until 4 consistent repetitions are achieved. Resistance is considered to be proportional to the amount of air that can be exhaled in one second, although this is dependent on the patient's level of effort, and if the effort is painful or tiring, or if the patient is too young to follow instructions properly, the maneuver may not be correctly performed [American Thoracic Society, 1994]. In whole-body plethysmography, a patient sitting inside a sealed chamber inhales or exhales through a flowmeter, while the movements of the patient's chest cause changes in chamber pressure that can be measured. Respiratory resistance is calculated using the relationship that resistance is equal to pressure change divided by the resulting flowrate. As in spirometry, the patient must be willing and able to perform breathing maneuvers that may be uncomfortable during illness [Holland, 1986].

In current clinical practice, however, because there is no appropriate instrument available, very little attention is given to airway resistance in patients so seriously ill that they cannot or will not comply with the standard techniques. Resistance is measured sporadically, if at all, in hospitalized people when the physician chooses to take it into account in a daily examination of overall health. He does this in unconscious and ventilated patients by performing an occlusion maneuver, that is, by shutting off their air flow for up to two seconds during an inhalation or exhalation, and measuring resistance by the ratio of the difference between occluded and unoccluded pressures to the change in flow [Abreau, 2001]. He may also employ an esophageal balloon in a related technique. This same calculation has also been performed using the 200-300ms delay caused by existing

ventilator valves as the occlusion period [Conti, 1998]. Stopping the breath of a conscious but weakly breathing or lightly sedated patient, however helpful the resulting information, causes extreme discomfort and thus is rarely done [Farre, 2001].

A newer method is applied to both conscious and unconscious patients by driving air at low pressure differential (generally less than 2cm H₂O) into the patient's mouth during normal breathing at a higher frequency than the breaths and measuring the pressures and flows as they exit the driving mechanism. This is called forced oscillation, and is an improvement over previous techniques since it requires no maneuvers from the patient, but is hampered by interactions in the soft palate and upper airways which flex unpredictably and elastically absorb some of the flow energy, interfering with the calculation [Navajas and Farre, 2000].

Johnson [1974] used a variation on the occlusion maneuver to create a continuous resistance monitoring device, in order to permit diagnosis of airway conditions without a complicated procedure that would discomfit an already sick individual. This device uses a rapid, periodic perturbation of air flow to compute airway resistance by measuring the ratio of the pressure change during the disturbance to the change in flow. Some conditioning of the signal is required since there are two components of the pressure change thus produced, one in-phase with the flow disturbance and one out of phase – the former is proportional to respiratory resistance [Vo, 1987]. Several studies have been conducted to validate this method and verify that it is not prone to the error induced by the flexing of upper airways seen in the forced oscillation technique (see Sahota [1980] for details).

Previously the flow disturbance mechanism used in this instrument, called the Airflow Perturbation Device (APD), was a rotating wheel with alternating resistance and non-resistance segments perpendicular to flow. A pneumotachograph and attached pressure transducers gave the needed flow and pressure signals – differential pressure across the airway was measured using the assumption that alveolar pressure does not change when the airflow is perturbed. Sahota [1998] showed that resistance measured by this method includes that of the entire airway from trachea to alveoli, and thus indicates the presence of any of the dangerous conditions previously discussed. This was verified by using accelerometers on the chest wall which were able to detect the waveform produced by the APD, in a study which also verified the device's ability to produce repeatable, resistance-proportional measurements [Lausted, 1999].

Unfortunately the current rotating wheel approach is not robust. Moisture collection in the system, a constant condition in ventilatory applications, can cause the wheel to hesitate or bind. High airflows slow the wheel audibly during maximum inhalation and exhalation. Vo [1987] attempted to design a replacement, specifically for use in series with mechanical ventilators, with a pinched tube, much like a roller or peristaltic-type pump, in which the occlusion is supplied by a cam with lobes of a shape carefully designed to produce the desired magnitude and periodicity. This system was deemed undesirable for further development, however, because of several mechanical problems including rapid wear of the tube, large size, prohibitive weight, noise, and the need for a substantial source of electricity.

If a new disturbance mechanism were designed so that the proven analysis approach of the APD could be successfully adapted for the physical demands of clinical use, the benefits to patients could be substantial. The ability to immediately and continuously visualize and analyze changes in airway resistance would supply physicians with the information necessary to diagnose not only immediately threatening situations such as a blood-filled airway, but also long-term degradations in airway status that point to a life-threatening and otherwise hidden breathing condition.

An important application of airway resistance measurement in ventilated patients has bearing on the problems of mechanical ventilators discussed in Section 2.1. If the APD could be adapted for use in series with ventilators, continuous monitoring of resistance would lead to the ability to predict with every breath the exact inlet pressure required to maximize lung volume without exceeding limits based on anticipated damage. Currently, the lung can be inflated only until inlet pressure reaches maximum safe pressure, since the head loss due to resistance is unknown, and the lung is never fully inflated. For the theoretical insufflation at constant flowrate pictured in Figure 1 below, P_{max} is the maximum pressure deemed safe for the lungs in. Ideally plateau pressure would be equal to P_{max} , but since $P_{resistance}$ is unknown, the entire curve must be kept under the P_{max} line. In cases of large resistance, the loss of lung inflation volume (tidal volume) is substantial.

Region A is the initial pressure increase at the inlet due to flow resistance in the airways. Region B is the constant-flow lung inflation opposed by the elasticity of the lung tissue and chest wall. Region C is the plateau pressure between the end of

inhalation and the beginning of exhalation, and pressure drops at the inlet since the need to oppose airway resistance is removed by lack of flow. The transition from C to D is the opening of the exhalation valve, allowing the inlet (mouth) to go to atmospheric pressure. In region D lung alveolar pressure declines exponentially as air is elastically expelled, opposed by exhalation resistance.

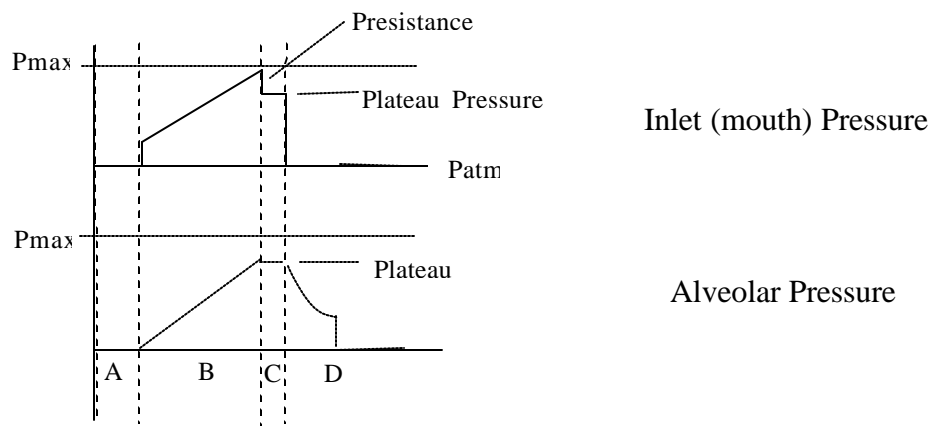


Figure 1: Reduction of Achievable Lung Pressure by Unknown Airway Resistance
 [Adapted from Hubmayr et al., 1990; Johnson, 1991; Martini, 1998; Aslanian et al., 199; and Kreit et al. 1994.]

2.3 The Role of Valve Design

The next step in the evolution of ventilators is a mechanical air flow control device that can improve both ventilators and the APD. In general, it can be said that standard valve types are not suitable for this type of activity for two reasons. One is

their long actuation time – the lengthy rotary motion required to close, for example, a globe or gate valve would be unacceptable in this setting. The other is general suitability to a medical application. The valve must tolerate high humidity, require little supporting equipment, be light and compact, and have excellent throttling characteristics. It must not contain or involve any materials hazardous to the respiratory system, and must use little or no lubricant, with complete isolation of lubricated surfaces from the air flow path, since these substances can be extremely harmful to the lung. The valve must either be disposable or capable of being sterilized if it is to come in contact with exhalation flow; current designs lack this quality, a long-ignored problem that has become critical during the present outbreak of SARS [Field, 2004]. In the current hospital financial environment, inexpensive production is also of capital importance.

One common type of valve used in medically-related air flow applications is a type of rotary shutter device called a scissor valve. In general it possesses the desired qualities, but it has poor throttling capabilities and requires substantial actuating travel that results in a lag between the initiation of motion and significant change in flow. Although concerns about litigation make all aspects of ventilator design highly guarded proprietary information, some ventilator companies will state that they employ this type of device [SensorMedics, Emerson, Puritan-Bennet, 2003]. Another design frequently advertised by valve-making companies as ideally suited for ventilator use is the proportional solenoid valve. These perform reasonably well, with the more expensive models capable of particularly high frequencies, but are prone to

hysteresis as great as 20%, which makes control a difficult problem [Kosarzecki, 2003].

A valve that could produce the flow changes necessary for the ventilator would also be well suited to replace the perturbation mechanism in the APD. The flow capacities are necessarily equal, and although it is mandatory that the APD device not close completely in order to ensure a patent airway for the patient at all times, a small modification to the valve or housing should be possible that would satisfy this restriction.

Recent improvements in the availability of smart materials have given rise to the possibility that one of these technologies might provide a solution to both the ventilator control valve problem and the APD perturbation challenge. The ideal approach would be to make a control device completely from a smart material with no other moving parts, but none of the substances currently in development combine the required strength, speed, and magnitude of deformation to produce such a mechanism. In conjunction with control surfaces like those used in existing valve designs, however, these new actuators could present a useful solution to limitations that have not seen a satisfactory alternative in existing valves. The properties that would make a valve highly compatible with smart material actuation – minimal travel and mass – are the very qualities that are sought in the improvement of ventilatory applications.

Ultimately, the ideal implementation of both a workable solution for resistance measurement and the reduction of valve lag time could lead to an integrated system in which real-time data regarding the patient's airway status is

provided to the physician who then sets the ventilator to an algorithm that provides the best gas exchange for the patient's immediate condition. With improved inspiratory and expiratory valves this program could be carried out more precisely, leading to results that more closely approach natural respiration, and resulting in reduced fatigue and damage to the patient. This goal is well within the capabilities of current electronics and software, and awaits only the appropriate hardware to become a reality. The most newly proposed methods of ventilator control, collectively called proportional assist ventilation or "power steering" attempt to use positive feedback to work toward this end, but even their most ardent advocates admit that their practical application awaits the necessary flow control device [Brunner, 2002].

Chapter 3: A Novel Air Control Device

This chapter describes an air flow control mechanism that overcomes the difficulties associated with current ventilator and Airflow Perturbation Device designs. The slow actuation seen in current mechanical ventilators is eliminated here by employing only a few moving parts of small size and low density. This method of flow control will also work well in the APD because it is not sensitive to humidity or flow nor does it bind during prolonged operation.

We will begin with a description of the proposed valve, and discuss its intended qualities which are to be tested experimentally.

3.1 Design

Figure 2 depicts the valve that was produced as a result of this work. It consists of four equal wedge-shaped sections that fit together to form a cylinder 25 mm in diameter and 10 mm thick, when closed. In the open position the these sections move apart to form an X-shaped opening 1 mm wide between pieces. This cruciate orifice is maintained by soft springs so that a symmetrical, circumferential force is required for the four wedges to move together. When that happens, each spring compresses into shallow wells cut into the flat opposing faces of the wedges. When the force is released, the valve springs open again to permit flow through the orifice.

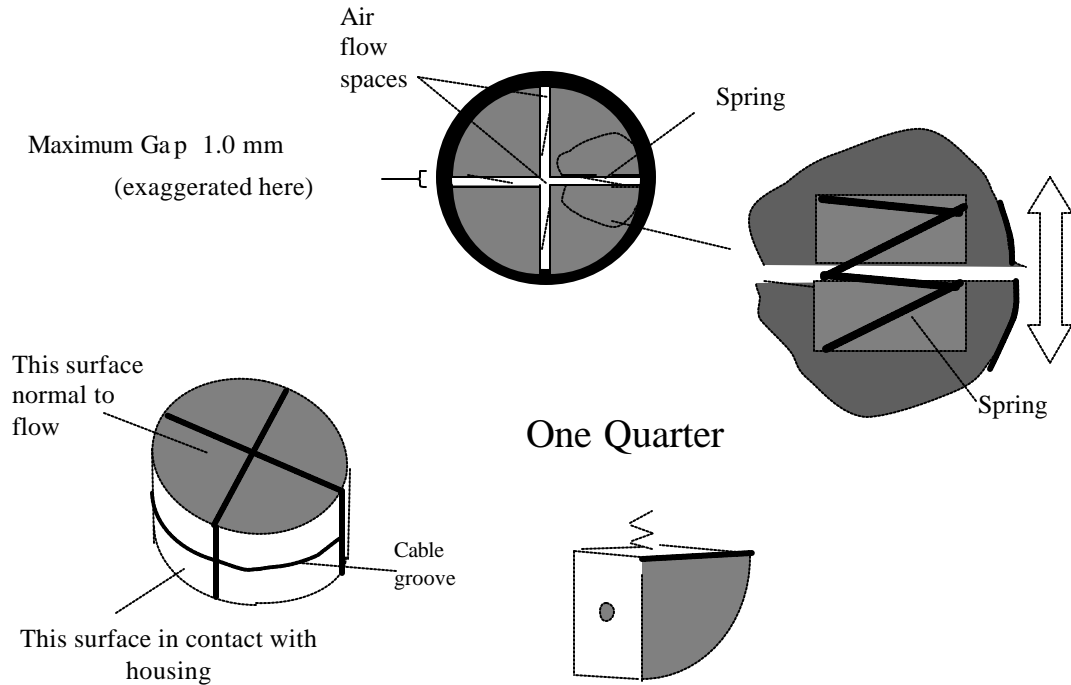


Figure 2: Design Concept

Figure 3 shows the final prototype used in the testing of this design, with the wedges arranged in a retaining ring. The cable used for actuation is not visible here, but wraps around the four wedges and passes out through a hole in the surrounding ring to attach to the motion-generating device. This is a small, high-frequency electric motor which wraps the cable around its axle to close the valve, or unwraps it in the opening direction, as it turns. In the future, however, this is intended to be a smart material such as an electroactive polymer in order to reduce the overall size and weight of the whole unit.



Figure 3: Internal Parts of Prototype Air Flow Control Device

The moving parts of the valve have a total mass of 4.90g, and the center of gravity of each wedge moves through 0.69 mm as the valve transitions from fully open to fully closed. These parameters result in a low-inertia valve that throttles or stops flow with a minimum of motion and therefore can be fully actuated within a very short period. The wedges are machined from Delrin®, a material chosen for its low density, toughness, and consistent composition; it is frequently used in medical applications and can be easily disinfected.

The springs are chosen for desired performance, balancing two needs: i) to minimize the force required by the actuator to shut the valve, and ii) to make the valve open rapidly and reliably in all conditions of flow. The springs used in the final prototype were made of 0.45 mm diameter silver-coated beryllium copper which was chosen for its high fatigue strength and ability to withstand corrosion in humid environments. Their spring constant was 0.53 N/mm.

The valve is actuated by a reducing its circumference by means of a ring or loop of cable placed around it. This could be an electroactive polymer ring that deforms in the presence of an electric field to produce the necessary diameter reduction. Testing showed that the state-of-the-art in these materials did not provide

adequate actuation force for this application, however. In its place, a polytetrafluoroethylene (Gore-Tex ®) cable was used, with the collapsing loop being formed by passing the free end through an eye in the portion wrapped around the valve. This choice of material resulted in low friction between the cable and valve body, allowing the valve to open with minimal spring force and producing quick actuation in both directions.

An adapter was fabricated to provide coupling with upstream and downstream tubing and provide lateral stability for the valve quarters in addition to closing the flow path at the valve gaps. A diagram and photo are shown in Figure 4. A paper ring is inserted between the valve wedges and the retaining ring in the photograph for visual clarity.

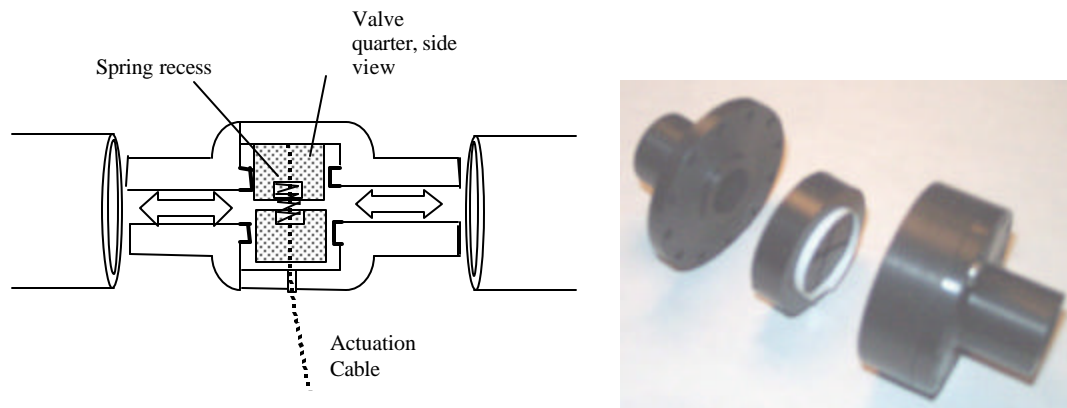


Figure 4: Diagram and Photograph of Valve and Housing

The housing was made in two parts in order to facilitate insertion and removal of the moving valve parts, and is clamped together by 16 custom-cut bolts around the perimeter. If tightened carefully these eliminate the need to use a gasket at this

closure, although at pressures above the range of interest to this work a more complex closure might be necessary. The size of the tubing extensions was chosen for compatibility with standard ventilator hose which can easily be ring-clamped to the housing with no significant leakage.

A lip was included where the flat faces of the moving valve parts slide against the housing at the inlet and outlet, because in the intended application moisture tends to collect along this surface and cause adhesion if the contact area is too large. Friction at this interface can be substantial, particularly when the valve is closed against a high pressure differential, and must be overcome with adequate spring and cable force. In the case of using the valve as the perturbation mechanism for the APD, one option for ensuring that the valve could never completely close off flow, guaranteeing that the patient would always have an open airway, would be to cut grooves into this lip, purposely allowing some air to leak around the valve seat.

Care was necessary in choosing the method of springing apart the quarters of the valve. The actuator would exert a constrictive force to bring the quarters together, but some other mechanism would need to be added to re-open the valve during actuator relaxation. The idea ultimately used was to employ compression springs with their ends recessed in opposing flat faces so that the quarters could close together completely if desired. In the case of using this valve to provide perturbation for the APD, a second idea for ensuring a flow pathway even if the valve failed shut would be to place stops between the valve quarters to keep them from lying flat against one another at maximum loop contraction. A further refinement was to include guides made of steel tubing through which the spring could be inserted, to

provide the desired stability and keep the valve quarters from fluttering. For the diameter of springs available, the enclosing tubes had approximately the same area normal to flow as the theorized spring shields used in the flow calculations in Section 3.2.

Simple wood prototypes were built for several other springing arrangements which ultimately were not as promising. Leaf springs connected at the perimeter of the valve across each inter-quarter gap would only negligibly constrict flow and could provide stability in the arrangement of the valve quarters by making them thick enough in the direction of flow to control any twisting motion caused by high velocities. The deformation of a flat spring at this location, though, would exert an outward force on the actuator. A closely related idea was to attach the quarters to the inner wall of a flexible rubber tube with the actuator wrapped around the outside of it, which would have the advantage of completely containing the airflow, an arrangement that might be desirable if vaporized medicines were to be introduced upstream of the valve which would tend to precipitate from the stream in regions of tortuous flow. The model showed that that this design, too, would have to be abandoned, because the deformation of the small amount of free tubing at the valve gaps produced a large amount of force, and this would unacceptably restrict the types of driving mechanisms that could be used. A third possibility was to pinch a very thin-walled latex tube into the gaps between the valve quarters, and use force exerted by the wedges on the outside of this conduit to produce deformation that would control flow. This, too, would have the advantage of allowing complete isolation of the air stream from the actuator of the valve, and in this case from the hard parts of

the valve as well, but the model showed that thinner latex tubing could not be made to spring open nicely when the valve was open, and that heavier tubing did not compress well to produce flow control. A fourth alternative was to use disc springs between each pair of valve quarters with a recess cut into one face of each to allow the quarters to close together completely. The prototype of this design worked well and held up under constant motion.

3.2 Geometry and Sizing

In order to understand the decisions made with respect to the shape and size of the proposed valve, it is necessary to keep in mind some important parameters.

Mechanical ventilators are designed to produce maximum flows of 120 L/min at a driving pressure of 120 cm H₂O. Flowrates in this range are generally associated with exercise and so this is ample for any patient resting quietly in a hospital bed or participating in basic respiratory testing in a physician's office; it is therefore also a reasonable limit for the APD. The target for actuation time was 200 ms or less since this is the figure generally quoted for the initiation of air flow control in ventilators.

We would like to improve that time by an order of magnitude or better.

Even though currently available electroactive polymers did not lend themselves to testing of the prototype in this project, we kept the actuation length within their operating range to facilitate later adaptation. This meant that the length change required of the actuator had to be 4% or less of its original length. If a better polymer does become available it will be enormously beneficial in this application

since it will be light and low-volume compared to an electric motor, and will require substantially less power to run.

3.2.1 Selection of Orifice Shape

Orifice geometry was the key to a workable design with minimal valve travel in order to improve time response. To satisfy the goal of minimizing valve motion it was necessary to find an orifice shape that would produce the largest change in area for a given change in perimeter.

For simple shapes, one can easily describe their change in area as a function of change in perimeter:

Circle:

$$\Delta A = \frac{1}{4p} \left(2p \sqrt{\frac{A_0}{p}} - \Delta P \right)^2 - A_0$$

Square:

$$\Delta A = \left(\frac{4\sqrt{A_0} - \Delta P}{4} \right)^2 - A_0$$

Square with two sides held constant:

$$\Delta A = \frac{-\sqrt{A_0} \Delta P}{2}$$

Equilateral triangle:

$$\Delta A = \frac{1}{18} (3\sqrt{2A_0} - \Delta P)^2 - A_0$$

Equilateral triangle with two sides held constant at $(2A_0)^{1/2}$:

$$\Delta A = A_0 \sin \left[\cos^{-1} \left(\frac{(\sqrt{2A_0} - \Delta P)^2}{-4A_0} - 1 \right) \right] - A_0$$

Rectangle with length to width ratio of a:1, long sides held constant

$$\Delta A = -a \sqrt{\frac{A_0}{a}} dP$$

Where, in the formulas above:

A_0 is the original area

ΔP is the perimeter change

ΔA is the resulting change in area

A graphical representation of these equations is included in Figure 5, using quantities representative of the dimensions needed for this control device.

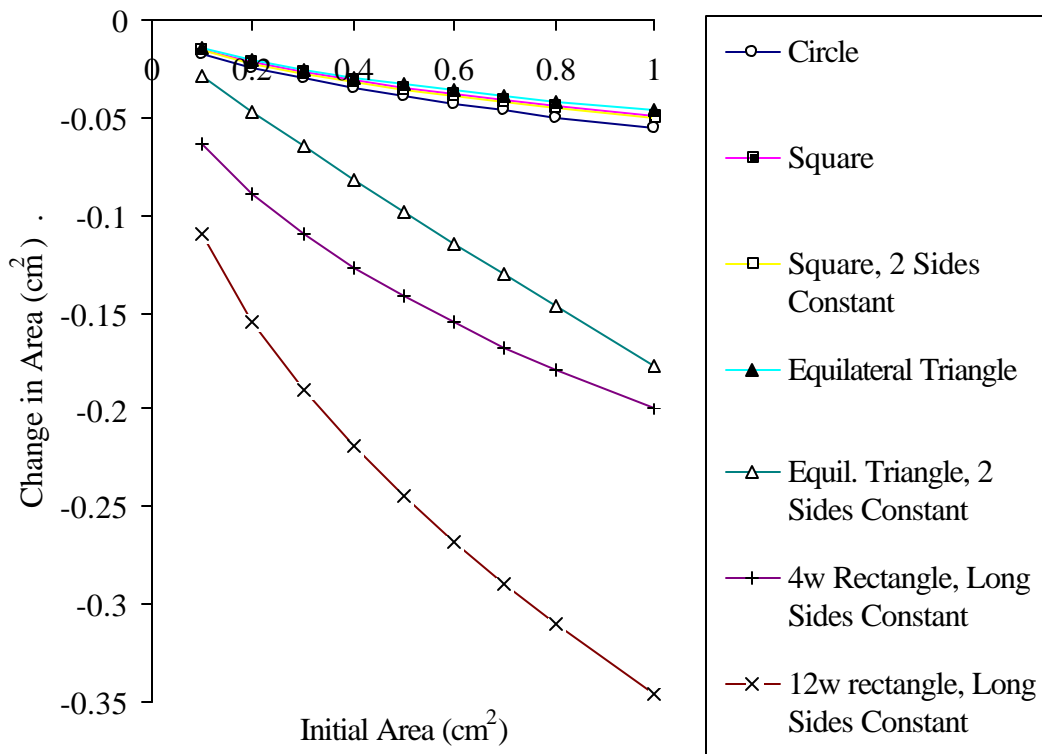


Figure 5: Relationship of Perimeter Change and Area Change for Orifice Shapes for a 0.1 cm Reduction in Perimeter

Most existing valves have an irregular orifice shape that is roughly circular or square, and thus require a large perimeter change for a given change in area and flow, as demonstrated in Figure 5. One exception is the globe valve, which has a conic

disk-and-seat arrangement that produces an approximately rectangular cross-sectional area for flow but requires very large stem travel in order to create a change. As Figure 5 shows, for a given perimeter change and initial area, the maximum reduction in area comes from the rectangle with its long sides held constant (each short side is reduced by $P/2$). The longer the rectangle compared to its width the better this performance. This observation is supported by the fact that the circle is the shape with the maximum ratio of area to perimeter, while thin rectangles have the smallest area to perimeter ratio.

The simplest way to employ this relationship was to create a circular valve with an X-shaped (cruciate) orifice, the arms of which would be four such rectangles that would change in width by the amount of reduction in the circular diameter. More arms in the orifice would amplify the change in area but would also complicate construction, and for a demonstration at this stage such a trade-off was considered undesirable.

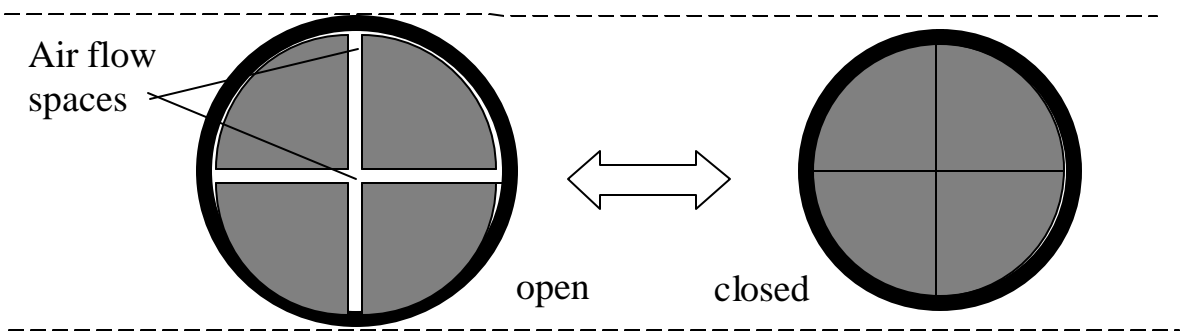


Figure 6: The Range of Valve Motion

To determine the feasibility of the proposed design, it was first necessary to determine whether an adequate flow area could be created while restricting the valve

gaps so that the valve could be fully closed with the intended 4% diameter change. A further constraint was the need to keep valve size moderate – for the target application, a valve more than a few centimeters wide is not acceptable. Minimization of valve size would also lower the mass of the moving parts, reducing their inertia and improving response time.

3.2.2 Required Airflow Capacity

The maximum area for flow (A_{max}) should be sufficient to allow 120 L/min of airflow with 120 cm H₂O upstream pressure, as discussed above. The differential pressure in an operating mechanical ventilator is reduced by the use of positive end expiration pressure (PEEP), in which a constant higher-than-atmospheric pressure is maintained in the lungs, even at maximum exhalation, in order to maintain recruitment of maximum lung tissue, in other words, to reduce the collapse of small airways leading to the problems discussed in Chapter 2.

For a rectangular orifice (as if the gaps of the cruciate orifice were laid-end-to-end, plus the open square at the center of the X), we assumed a length to width ratio of 6:1, so that for the rectangular orifice described above, area (A) = $4lw + w^2$, and perimeter (β) = $8l + 4w$. The following equations predict the required flow area [Munson et al., 1994, p505]. The hydraulic diameter is

$$D_h = \frac{4A}{\beta} = \frac{4(4lw + w^2)}{8l + 4(0.5w) + 2w} = 1.923w \quad (1)$$

The differential pressure across the orifice is given by

$$\Delta p = f \frac{L}{D_h} \rho \frac{v^2}{2} \quad (2)$$

where f is the Darcy friction factor, L is the length in the direction of flow, D_h is the hydraulic diameter as calculated in (1), ρ is the fluid density, and v is the mean velocity of the fluid. For circular conduits, the Darcy friction factor may be read from a standard graph, but for a rectangular orifice it must be calculated from a constant (C) that is related to geometry ($C = 96.0$ for a rectangle with length to width ratio greater than 20:1) and the hydraulic-diameter-dependent Reynolds number (Re_h) which is calculated from density (ρ), velocity (V), hydraulic diameter (D_h), and the fluid viscosity (μ) as follows:

$$f = \frac{C}{Re_h} = \frac{C\mu}{\rho V D_h} \quad (3)$$

We can combine Equations 1-3 to obtain:

$$\Delta p = \frac{C\mu L Q}{A D_h^2} \frac{1}{2} \quad \text{and therefore} \quad A_{\max} \geq \frac{C\mu L Q}{2\Delta p D_h^2} = \frac{0.425}{w^2} \quad (4)$$

where w is in mm and A_{\max} is in mm². This result is obtained knowing that the flowrate (Q) is equal to the velocity multiplied by the area for flow, the driving pressure is (120-5) cm H₂O = 11.3 x 10³ N/m², the length in the direction of flow is 0.01m for reasons that will be explained shortly, and the viscosity of air is approximately 1.85 x 10⁻⁵ N.s/m². Equation 4 tells us that we can choose a suitable width (w), and the minimum area to produce the given flow will be given by this ratio. It is clear that the required area should be dependent on the width, since Equations 1-4 attempt to take into account the friction of the fluid against the orifice

wall, which will necessarily change with proportions. For a less favorable pressure head, once lung pressure reaches an average value of 15 cm H₂O, the minimum orifice area is given by $0.465/w^2$, if 120 L/min airflow is still desired.

Since Equations 1-4 only place a restriction on the orifice proportions, and do not determine the actual flow area required, a simple Bernoulli analysis was performed. The assumptions are that air flow in this region is inviscid, steady, and sufficiently laminar so that streamlines are consistent in moving through the valve. An additional assumption is that the air is incompressible, since in this region the compressibility corrections are minute compared to the remainder of the terms. The streamline in question would be at a constant or nearly constant height, and the gravity term would be very small. The points chosen for analysis are just upstream of the valve and just inside the valve on the downstream side. These simplifications leave us with $h_L = K \frac{v^2}{2G}$. For existing valves the value of K is well known and can be found from design tables, but in our case it must be estimated. For the most restrictive configuration in the tables (gate valve 1/4 open), $K = 20$ [Welty et al, 1984].

The continuity equation, $Q = VA$, combined with the Bernoulli solution, using an air density of $\rho = 1.2928 \text{ kg/m}^3$ gives the head loss as a function of flowrate and area as

$$h_L = 20 \frac{\frac{Q}{A}}{2(9.81)} = \frac{1.02Q}{A} \text{ and therefore } \Delta P = h_L Gr = \frac{12.68Q}{A} \quad (5)$$

where A is the cross sectional area for flow in m^2 . Therefore to allow the maximum flowrate of 120 L/min or $0.002 m^3/s$ with a minimum differential pressure of 20 cm H_2O (1.96 kPa), we require $A_{max} = 0.129 cm^2$.

In the determination of valve dimensions, which will be made in Section 3.2.3, both the rectangular conduit result and the Bernoulli solution need to be taken into account.

3.2.3 Determination of Valve Dimensions

Since the actuator is intended to operate in the constricting direction only, some method of opening the valve quarters is needed. We assume that this would need to be screened from the flow of air to prevent flutter, leaving a length l only of the orifice for flow:

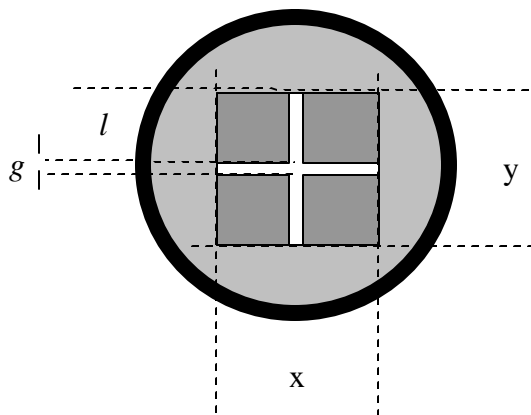


Figure 7: Assignment of Variables for Valve Calculations

For the partially occluded orifice shown in Figure 7, we conservatively assume that the spring screen moves with the other portions of the valve. The change in flow area as a result of a change in the overall circular diameter is $\Delta A = y_1\Delta D + x_1\Delta D + \Delta D^2$, where $\Delta D = \Delta x = \Delta y$. If we wish to change the area from the closed area $A_0 = 0$ to the open area A_{max} , we require an increase in diameter ($?D$) given by:

$$A_{max} = \Delta A = 4l\Delta D + \Delta D^2 \quad (6)$$

If we are to achieve this with a given percent change (p) in the perimeter of the valve, for the change in diameter from an initial value of D_0 , we have $?D = D_0 \cdot p/100$ so

$$A_{max} = 4l \times \frac{D_0 p}{100} + \frac{D_0^2 p^2}{10^4} = \frac{D_0 p l}{25} + \frac{D_0^2 p^2}{10^4} = \frac{400 p D_0 l + D_0^2 p^2}{10^4} \quad (7)$$

and for the desired 4% travel, i.e. $p = 4$

$$A_{max} = \frac{1600 D_0 l + 16 D_0^2}{10^4} = 0.16 D_0 l + 0.0016 D_0^2 \quad (8)$$

or, in terms of g and l :

$$A_{max} = 4gl + g^2 \quad (9)$$

Assuming that the diameter of the closed valve would be equal to $4l$, that is, half of each quarter of the cruciate orifice would be blocked, for the open diameter D_1 , we have

$$D_1 = 1.04 \times 4l = 4.16l \quad (10)$$

Substituting into Equation 8, we can solve for the length l (and therefore for D_0) given the desired airflow A_{max} . For our previously calculated values of $A_{max} = 0.129 \text{ cm}^2$ (Equation 5), we find that $l = 0.625 \text{ cm}$ and therefore that the gap size ($?D$) given by Equation 9 should be 0.182 mm . To avoid the time and financial cost of re-

machining, we overdesign the valve to accommodate an A_{max} of 0.25 cm^2 with a gap size of 0.1 cm . Using Equations 8 and 10, this gives $D_0 = 2.5 \text{ cm}$ and $l = 0.625 \text{ cm}$.

We chose of valve height of 1 cm in the direction of flow. The longer the valve in this direction, the greater the minimum head loss it will produce when in the open position, which would be undesirable in most settings. On the other hand, if the valve is too short the sections of the valve might flutter or twist in conditions of high flow. This would produce unpredictable throttling, and would also create the risk that the quarters would become disengaged from one another and that they or the springing mechanism would be carried downstream and could harm ventilator or the patient.

3.3 Prediction of Flow Performance

In order to determine whether the proposed valve shape is suitable for use in ventilator and resistance measurement airflow control, we calculated the expected flow performance of the valve as a throttling mechanism and in response to a periodic input.

3.3.1 Throttling Characteristics

For the configuration described above, we assumed that the mechanism used to screen the springs from flow would remain attached to the valve wedges such that the length of each orifice quarter would remain constant at l . The throttling equation relating diameter change to area change (D) and the closed diameter of the valve (D_0) is:

$$\frac{dA}{dD} = 4l + 2D - 2D_0 \quad \text{and therefore}$$

$$\frac{dA}{dD} = 2D - 4l \tag{11}$$

where D_0 is the closed diameter and is equal to $4l$. As an example, this relationship is plotted below for a valve with $l = 0.5\text{cm}$, so that $D_0 = 2\text{cm}$:

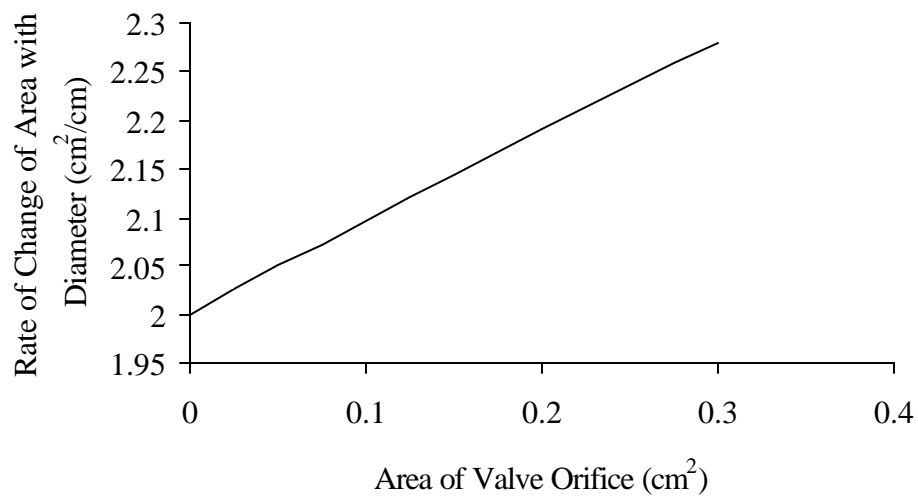


Figure 8: Predicted Throttling Performance of the Valve

This is precisely the relationship that is desired. Diameter change produces a linear increase in area.

This is borne out by a similar plot of predicted flow versus valve movement in Figure 9:

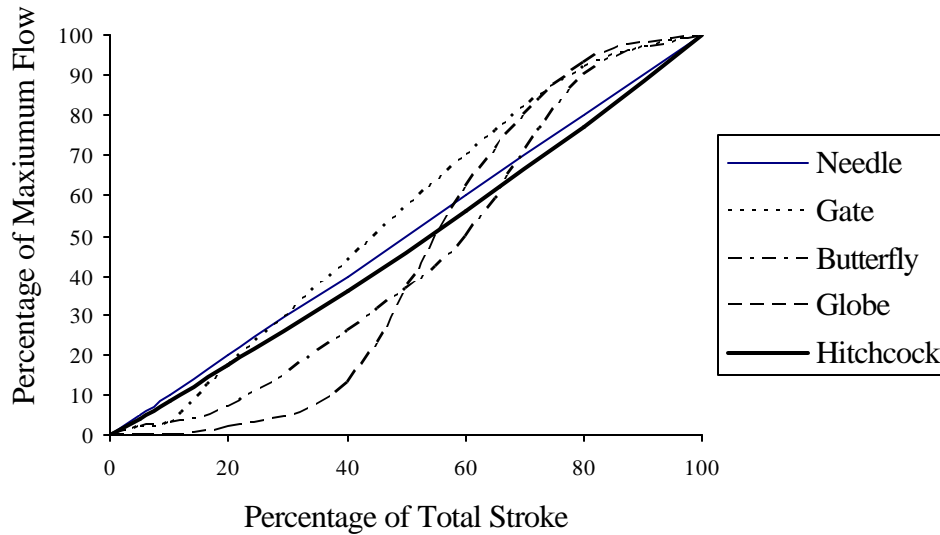


Figure 9: Comparison of Theoretical Valve Performance with Major Valve Types
 [Adapted from Zappe, 1981; and Lyons, 1982]

In Figure 9, the line for our proposed design is drawn based on the assumption that flowrate is directly proportional to flow area at constant upstream pressure (Equation 5). As shown in this graph, the designed valve does not possess the optimum throttling ratio of the globe valve between 40% and 60% of stroke, yet it has a linear flow vs. stroke relationship without any regions of sudden change as seen in the gate valve. This would be an important advantage if the valve were used as part of a feedback control system.

3.2.2 Expected Response to Periodic Actuation

In both the APD and mechanical ventilators, current methods of use show that the valve would need to respond across its range of flow at a rate of 10 Hz or better. Implementation of the proposed design would depend on ensuring that this rate of operation is far from the natural frequency of the system, and on finding a driver with

sufficient force or torque to produce the desired displacement at the needed frequency. The natural frequency of the system of a single valve wedge of mass m and its associated spring with constant k is:

$$\omega_n = \sqrt{\frac{k}{m}} = \sqrt{\frac{5256N/m}{4.90 \cdot 10^{-3} kg}} = 1036Hz \quad (12)$$

To calculate the natural frequency for the valve as a whole, it is necessary to determine the effective spring constant (K_{eff}) for the system. The mechanical work done to close one of the four gaps between the wedges from a starting gap width of g , knowing that the necessary force is $F = k\Delta g$, is given by $W = \frac{1}{2} F_{max} g_{max} = \frac{1}{2} k g^2$.

Therefore, for the system of four wedges, the work to close the entire cruciate orifice is

$$W = 4 \left(\frac{1}{2} k g^2 \right) = 2k g^2 \quad (13)$$

In order to determine the needed force to produce this work at the cable, we assume that the distance-force relationship is linear (which will be proven shortly). Thus, at the cable, the linear displacement S of the free end is given by the change in circumference ($p \cdot g$), and the work (W_c) performed on the cable is:

$$W_c = \frac{1}{2} p \cdot g_{max} F_{max} \quad (14)$$

Finally, since the work on the valve must be equal to the work at the cable, we can write

$$F_{max} = \frac{4k g_{max}}{p} \quad (15)$$

Equation 15 holds at any intermediate position, so F is a linear function of S as assumed above. The effective system spring constant can thus be calculated (using $F = K_{eff}S$):

$$K_{eff} = \frac{4k}{\mathbf{p}^2} \quad (16)$$

so the natural frequency is:

$$\mathbf{w}_n = \sqrt{\frac{4 \times 5256 \text{ N / m}}{4(4.90 \times 10^{-3} \text{ kg})\mathbf{p}^2}} = 330 \text{ Hz} \quad (17)$$

Armed with this result, we can calculate the force that must be produced by a motor attached at the cable to drive this valve in the necessary motion. The equations of motion are:

$$\begin{aligned} \ddot{x} &= \frac{-1}{M} K_{eff} \Delta x + \frac{F}{M} \\ \Delta x &= \mathbf{p}S_{\max} (1 - \cos \mathbf{w}t) \\ \dot{x} &= \mathbf{w}\mathbf{p}S_{\max} (\sin \mathbf{w}t) \\ \ddot{x} &= \mathbf{w}^2\mathbf{p}S_{\max} (\cos \mathbf{w}t) \end{aligned} \quad (18)$$

In order to produce a sinusoid that takes the valve from shut at $t = 0$ to a peak in which it is fully open, we require

$$F = M\mathbf{w}^2\mathbf{p}S_{\max} \cos \mathbf{w}t + K_{eff}\mathbf{p}S_{\max} (1 - \cos \mathbf{w}t) \quad (19)$$

in which x is the displacement of the cable from the open (neutral) position, M is the overall valve mass, \mathbf{w} is the angular frequency, and t is time.

Using Equation 19, it is possible to calculate the torque that must be produced by a motor in order to drive the valve along the desired sine wave. For this calculation it was assumed that the cable would be allowed to wrap around the motor axle itself rather than using a beam to amplify motor motion, so the distance that must be combined with the cable force to calculate load torque is the radius of the motor axle (r). Using the equations above, and the knowledge that the torque used to accelerate the motor itself is given by the derivative of the angular speed ($\dot{\mathbf{q}}$) multiplied by the rotational inertia of the motor (J_{motor}), we have a torque t given by

$$\mathbf{t} = \left[M \mathbf{w}^2 \mathbf{p} l_{\max} \cos \mathbf{w}t + K_{eff} \mathbf{p} l_{\max} (1 - \cos \mathbf{w}t) \right] \cdot r + \frac{3\mathbf{p}}{2} \mathbf{w}^2 J_{motor} \quad (20)$$

A typical small motor used in medical applications has a motor constant (K_t) of 0.27 oz-in/A and a rotational inertia (J) of 6.81×10^{-5} oz-in-sec², with a rotor diameter of 3 mm. For purposes of illustration, it was assumed that 150 Hz would be a frequency higher than any used in practical tests, and thus could represent an upper boundary on the operating range. Using the previously discussed valve parameters, we have:

$$F = (1.96 \times 10^{-2} \text{ kg})(0.001 \text{ m})(\mathbf{p} \mathbf{w}^2 \cos \mathbf{w}t) + \frac{4(5256 \text{ N/m})}{\mathbf{p}^2} (1 - \cos \mathbf{w}t)(\mathbf{p} \times 0.001) \quad (21)$$

This has minima where $\cos(\mathbf{w}t) = 1$ and maxima where $\cos(\mathbf{w}t) = -1$, so for the maximum force, at a frequency of 150 Hz, F is 12.00 N and acts at the motor axle radius of 1.5mm so that t_F is 2.54 oz-in (0.018 N-m), t_{motor} is 7.22 oz-in, and the maximum current needed at any time is $I_{\max} = 2.64 \text{ A}$ which is well within the safe operating current of the motor [Aveox, 2004].

The design described above should satisfy all of the objectives of this study. With the given mass and spring constants, the spring-and-wedge system would have a natural frequency that far exceeds the intended rate of operation. A stock motor would have the required torque to drive the valve throughout its desired frequency range. Flow calculations for this geometry show desirable throttling characteristics, particularly a gradual transition between full and zero flow.

In addition, the valve is sturdy and simply made which fits the requirements of the hospital environment. It can be easily disassembled for sterilization or replacement of internal parts, and the 100% humidity seen in ventilatory applications will not disturb it. The materials used are all known to be medically safe. In applications such as the APD in which total valve closure must be prevented as a failsafe, the design can be readily and inexpensively adapted to ensure that flow is always available.

Chapter 4: Experimental Setup and Procedure

This chapter details the instrumentation used, testing done on the throttling behavior and dynamic flow performance of the valve, and the use of the valve for flow resistance measurement.

4.1 Equipment and Instrumentation

Three different experimental setups were used to test the proposed design. The first was intended to minimize flow disturbances so that highly accurate calibration curves could be obtained without the influence of turbulence. The second was arranged to simulate the actual flow environments of the valve within a mechanical ventilator. The third was the standard setup for human testing of the APD. Similar instrument arrangements were used in all cases. The details of each are described here.

4.1.1 Apparatus

For static testing, a test chamber was built using 318 mm inner diameter, 3.2mm wall-thickness hard polyethylene tubing, with a length of 150 cm to allow air flow to become steady and laminar before entering the test section. At the inlet of the chamber, 0.6 cm diameter Tygon® tubing connected it to an air manifold supplied by the regulator described above. Near the outlet of the chamber a 2.5 cm inner diameter latex rubber tube was placed to keep the valve wedges immobile and form a seal around their perimeter so that accurate flow measurements could be made. The latex tubing was 25 cm in length, greater than the seven times its diameter as indicated by

the thumbrule for laminar flow, in order to allow the disturbance caused by the step-down in diameter at its inlet to be dispelled before the air entered the valve. The valve was placed at the downstream end of the tubing, which protruded slightly from the chamber to provide coupling with the pneumotachograph.

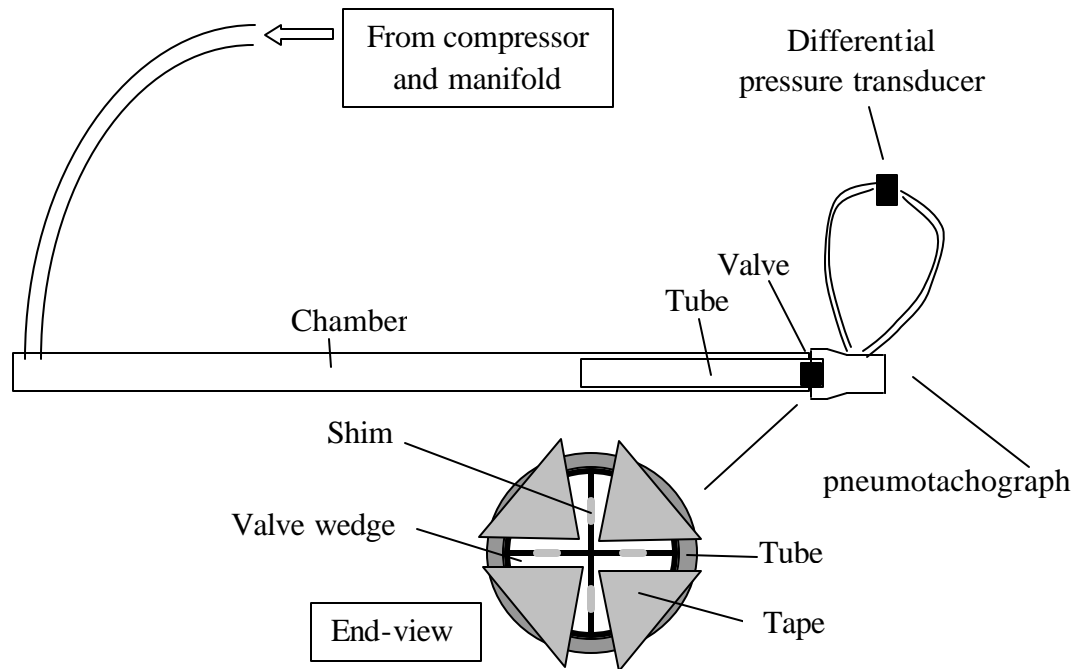


Figure 10: Static Testing Rig

For dynamic testing, the operational environment was simulated as shown in Figure 11 below. In these trials the spring-guides were removed since it was discovered that valve stability was adequate without them, and their presence added undesirable inertial and frictional effects. As shown in the diagram, airflow was supplied by the same compressor and reducer arrangement as in the static tests. In this case a 10 cm run of Tygon tubing was inserted between the valve and the

pneumotachograph in order to simulate the tubing between the control valves and the flow detector in a mechanical ventilator.

The actuation mechanism for frequency response testing consisted of a waveform generator with a signal fed through a power supply to an electric motor and gear assembly as shown below. This drove a lightweight aluminum arm with a Gore-TEX® cable attached at its end and wrapped around the valve body in a free-sliding loop. For step-input testing the motor used did not produce adequate torque, so the strike of a hand-held plastic rod against the motor arm was used.

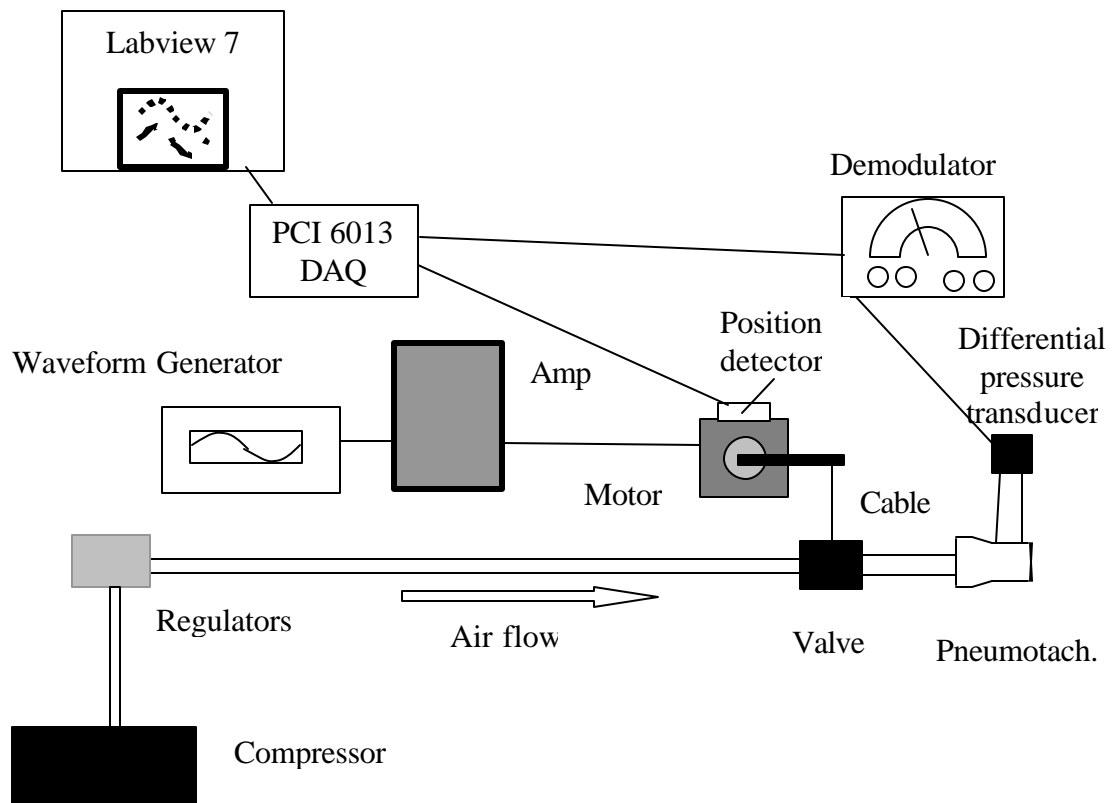


Figure 11: Dynamic Testing Rig

For dynamic testing, the valve was placed downstream of the Airflow Perturbation Device, as shown in Figure 12, and the built-in perturbation mechanism, a rotating wheel, was disabled in a position that left the flow path to the valve unobstructed. The valve was then removed and the wheel was to provide reference tests under the same conditions.

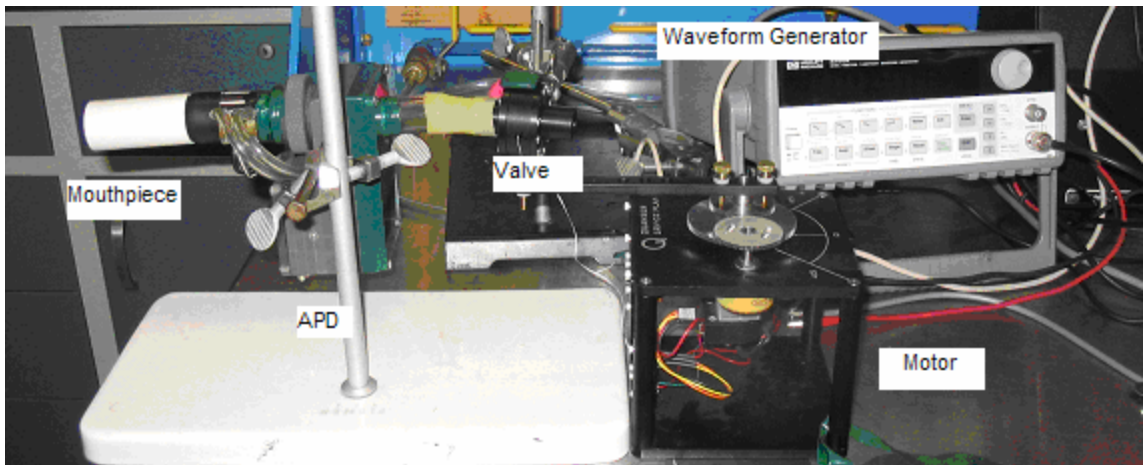
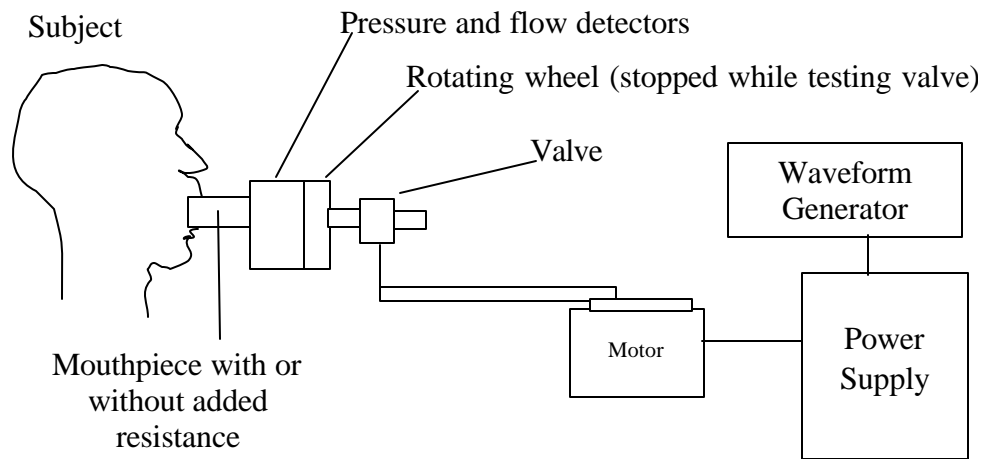


Figure 12: Apparatus for Resistance Measurement

4.1.2 Instrumentation

Air pressure was supplied to the testing rig by an electrically driven compressor followed by three reduction stages to minimize fluctuations. During static testing a two-arm water manometer and two-arm mercury manometer were used to measure the pressure supplied to the testing setup, and were read to 0.1 cm on each arm. For speed of reading during dynamic testing, pressure was measured using the reducer scale in units of psig and accurate to ± 0.1 psig.

Flow was measured using a Fleisch #3 pneumotachograph ($\pm 0.5\%$ of reading) purchased from Phipps and Bird of Richmond, VA, connected downstream of the test section holding the valve, its downstream end open to atmosphere. (The APD uses a Fleisch #2 pneumotachograph with the same accuracy). A Validyne (Northridge, CA) DP-15 pressure transducer (± 0.35 mV/V) was connected across the taps of the pneumotachograph for flow measurement via differential pressure using the factory-tested differential pressure versus flowrate calibration curve. During static testing the signal from the pressure transducer was converted to a 0-10V dc signal using a lab-built demodulator that was read using a Fluke 73 digital multimeter ($\pm 0.3\%$ of reading). During dynamic testing the signal from the pressure transducer was sent to a Validyne Carrier/Demodulator Model CD12. Processed output was fed to a National Instruments (Austin, TX) PCI-6013 type data acquisition card driven with NI DAQ 7.10 and graphed using National Instruments' Labview 7.0. Sampling occurred at 250 Hz. Calibration of the differential-pressure

signal was performed before each experimental run using a water manometer read in units of 0.1 cm.

4.2 Experiment One: Static Tests

Because the orifice of the valve is of a shape not previously investigated, its static pressure-flow relationship was first determined in order to characterize the valve's ability to throttle and finely control airflow. Polyester shims of graduated thicknesses were inserted into the spaces between each pair of wedges to form a cruciate orifice with arms of exact width. Each shim was circular in cross section with a diameter of 4 mm perpendicular to flow to equal the portion of the spring guide that would be exposed were the valve in the given position during dynamic testing, and centered on the opposing face of the wedge as the spring guide would be.

Shims with thicknesses of 0.10, 0.25, 0.38, 0.51, 0.64, 0.76, 1.02, and 1.27mm were used. Soft vinyl tape was used to hold the wedges in place at the mouth of the latex tube and prevent leakage between the tube and the curved surface of the wedge. The tape was carefully cut to the same shape as the wedge face to prevent occlusion of the orifice and a resulting reduction in flow. For each set of shims, flow through the valve was measured at upstream pressures of 1.7, 27.6, 53.2, and 79.6 cm of water as measured by the water manometer, and 73.4, 93.8, 111.5, and 127.8 cm of water using the mercury manometer (mercury heights of 54, 69, 82, and 94 mm).

Additionally, leak testing was performed on the assembled but unconnected valve quarters to determine whether flat, smoothly machined Delrin® faces opposed with minimal force would be adequate to completely stop flow. This test was

performed at the pressures shown above which represent the maximum range of pressures used within a mechanical ventilator. Flow could be completely stopped using the valve as built, so although at higher pressures it might be desirable to develop this aspect of the design, this simple approach is satisfactory for the intended purpose.

4.3 Experiment Two: Dynamic Tests

Upstream pressures of 0.5 to 7.0 psig were used to measure the response of the valve in closing against 0.53 N/mm springs. In order to simulate as nearly as possible a step-input to the valve, the motor arm was struck with a plastic rod to drive the valve fully shut during each trial. Aluminum stops were used on either side of the arm to ensure that motion did not exceed the desired range. The motor assembly was left attached, despite the undesirable small addition of rotational inertia, to provide position indication for the valve arm.

In order to further verify the ability of the valve to fully open or close in a desirable timeframe, a constant upstream pressure of 2.0 psig was supplied and waveforms at various frequencies were input via the power supply to the motor to determine whether full-range flow could be attained. A light latex band was used to counteract the tendency of the motor to continuously wind in the positive direction. Metal stops were again used to ensure that the motor did not over-expand the valve or snap the driving cable. These tests had to be discontinued at a maximum of 18 Hz because the motor had exceeded its maximum safe input voltage range.

4.4 Experiment Three: Resistance Measurement

Finally, the valve was used in place of the existing perturbation mechanism for resistance measurements. Two individuals were tested for natural breathing resistance and with a selection of four orifices placed between the subject and the resistance measurement device to simulate degraded ventilatory conditions. This procedure was validated in an earlier experiment [Lausted and Johnson, 1998]. The valve was driven at 10Hz during these trials, which is within the previously established operating frequency for the APD. The measurements were compared to those using the standard wheel-perturbed APD, for which the perturbation was nominally 11 Hz.

Chapter 5: Results and Discussion

The throttling performance of the valve matched the general predictions made for its performance, with a few important differences. As shown in Figure 13, the maximum desired gap size for the valve (1.00 mm) did not exactly produce the desired flowrate (120 L/min) at the maximum supply pressure for a mechanical ventilator (120 cm H₂O). With slight modifications to the valve dimensions, though, this flowrate would be easily achieved, and in fact was demonstrated using a slightly larger gap size of 1.27 mm.

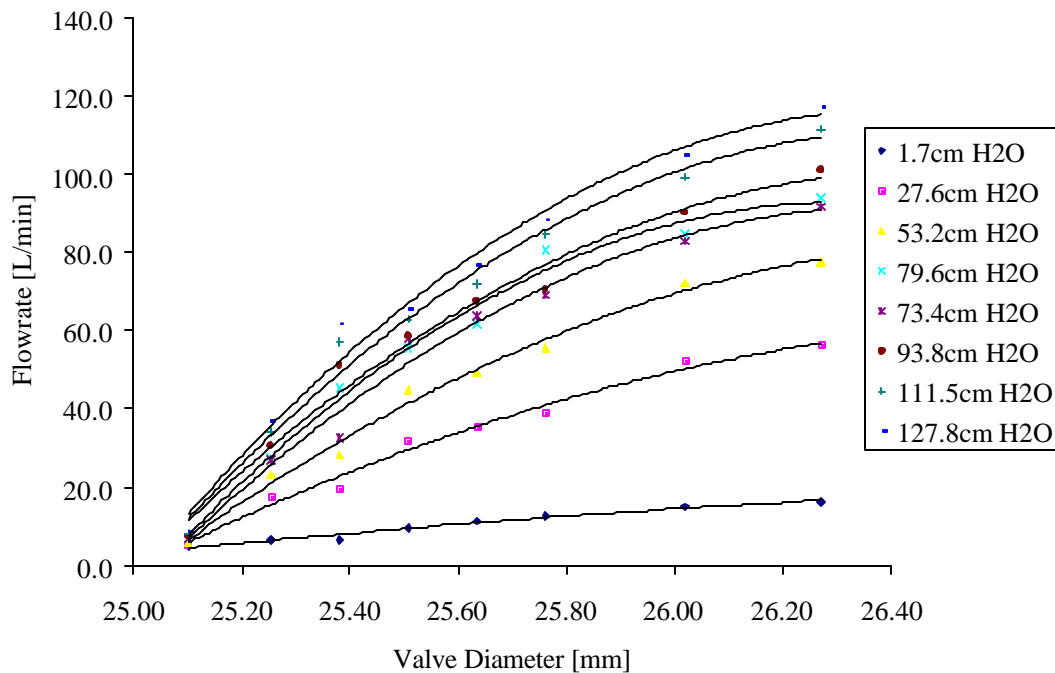


Figure 13: Flowrate as Function of Changing Gap Size

Lines of Constant Pressure

The curves as shown in Figure 13 could be used to produce valve-control software within a mechanical ventilator that would deliver exactly the desired flow to a patient as determined by the desired ventilation scheme. This graph demonstrates that very little motion is required in this design to produce substantial change in flowrate, even at the lower end of the pressure range used in ventilators. These lines become straight (least squares method fit of $R^2 = 0.93$) if flow is graphed as a function of flow area, as predicted by standard orifice flow equations. Those equations also show that flowrate varies as the square root of differential pressure across the orifice, and that too is demonstrated by these curves in the appropriate format.

An interesting difference from the theoretical predictions was the altered shape of the stroke versus flowrate curve generated by the static testing data in the appropriate format as shown in Figure 14. The actual performance shown here is the trend-line across all trials, since this relationship is consistent across the range of differential pressures.

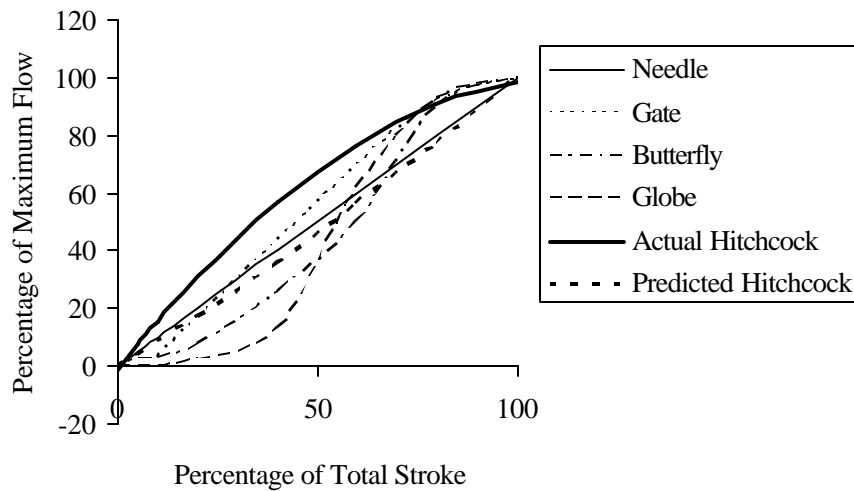


Figure 14: Actual Performance of Valve

[Adapted from Zappe, 1981; and Lyons, 1982]

This actual curve shape is slightly less desirable than the predicted one since in the nearly-closed region a small amount of valve stroke produces a greater change in flow. The reason for this is unknown but is almost certainly a function of valve geometry. Calculations were done assuming that the orifice is a rectangle, since that is the only shape for which equations are available that take friction into account. This valve incorporates an open square at its center with little friction, since its sides are the open arms of the X-shape, and this will necessarily have an impact on flow. This curve is still a consistent, predictable relationship without any sudden transitions, however, and is therefore still favorable for the intended uses.

As mentioned previously, the static testing did also demonstrate that a simple flat-machined surface at the interface between valve wedges was adequate to control pressures in excess of maximum ventilator pressure. This means that mass production of the valve with this simple wedge shape could be carried out cheaply

due to minimum design and machining costs, and that the hard, inexpensive plastic used in production would be appropriate for the actual application.

Simplicity of shape and production is important for two reasons beyond unit cost. In the resistance measurement application, the valve must have the ability to be sterilized between patients. This means either heat or chemical treatments in which every part of the valve must be accessible to steam, mist, or radiation. The only alternative is to make the internal parts of the valve disposable, which means that it must be easily disassembled and reassembled. Keeping the seat design simple promotes both ends.

The tests of the flow relationships during valve motion produced much better results than expected. In the absence of complete knowledge about the time-scale of current ventilator valve designs, due to careful guarding of that information by the companies that produce these machines, a goal of 200ms or less was set and exceeded for these trials.

The compilation graph shown in Figure 15 was made by examining flow and valve motion plots at each pressure, and extracting just that part of the graph in which the motion of interest takes place. Each line was time-correlated to the valve motion included in the graph so that the exact time from start of valve motion to beginning of flow change is shown here.

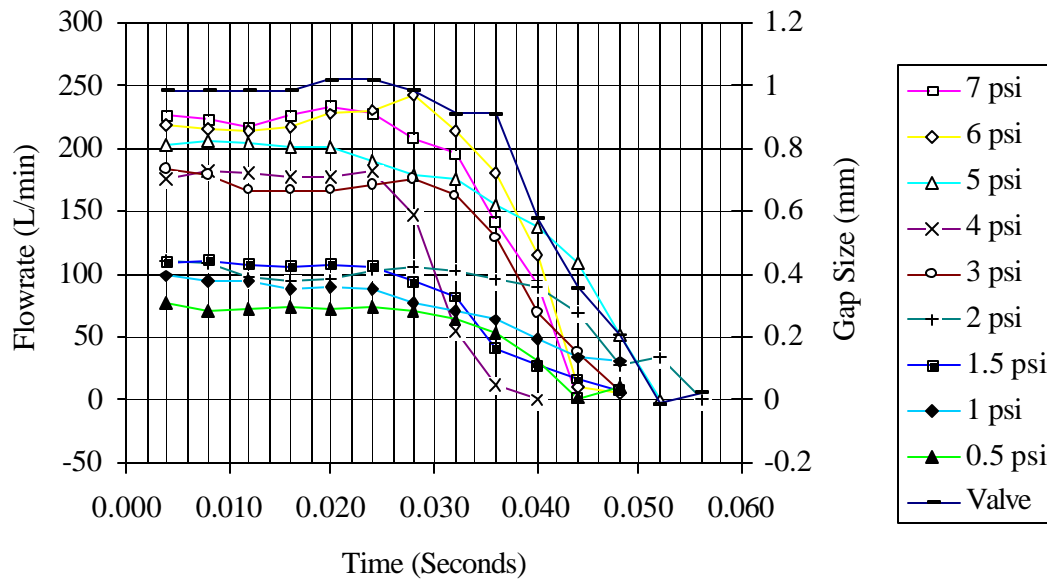


Figure 15: Step Input to Valve, Closing

Sampling in Figure 15 is at 250 Hz, and each symbol represents one sample. Each line shows the motion of the valve from 1mm gap size (valve diameter = 2.60 cm) to fully closed or vice versa. As is apparent here, the equipment used to measure flow was at the limit of its ability to respond on this time scale, but these curves nevertheless show the expected characteristics. It is interesting to note that higher differential pressure across the valve did not result in slower closing response as might be expected. It is also of interest that the motion of the valve did not appear to cause large disturbances in the flow even at the lower pressures, as the lines remain equally smooth across the differential pressure range.

The valve fully closed in 28 ms or better throughout the trials represented by this graph, despite valve motion which required an equal amount of time. This is

attributable to the extremely small amount of motion required to change flow across the full range, in comparison to existing designs which require substantial linear or rotary action to produce a needed change in flow area. The moving parts of this valve are also very few and have low mass, so the required force is small and acceleration is rapid.

These conclusions are reinforced by the results of the trials in which a signal of constant frequency was used to drive the valve between full flow and no flow at a differential pressure of 2 psi, shown in Figure 16.

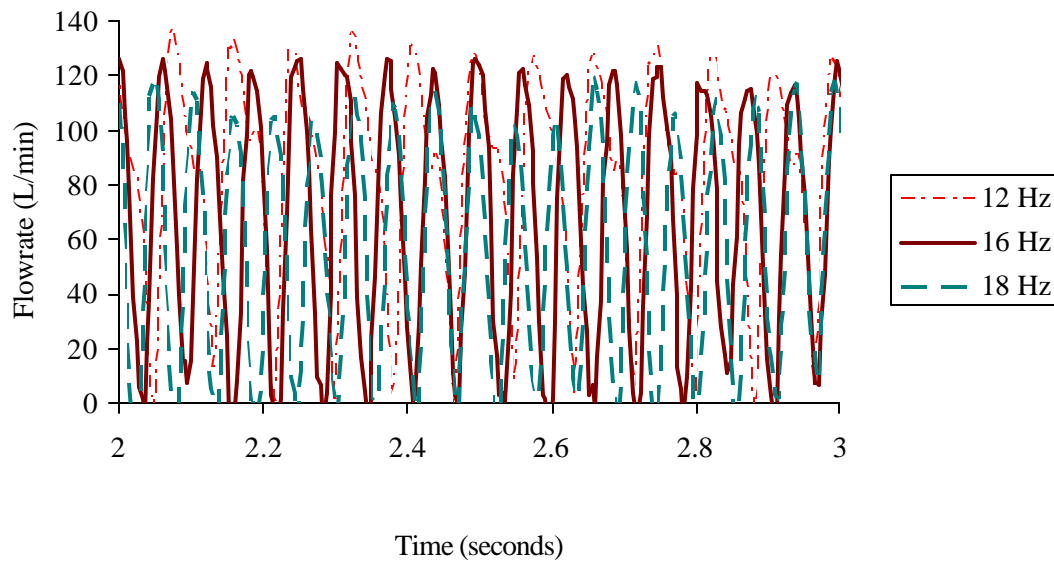


Figure 16: Valve Response to High Frequencies

As shown here the valve was demonstrated to produce full flow changes at up to and including 16 Hz. The results of the step-input trials suggest that even higher frequencies would be possible, but even at 18 Hz, as shown in Figure 16, the voltage input to the actuating motor could not be made large enough to cause full range motion without damaging the motor system. Nevertheless this graph does support the step input data, and demonstrates that many full actuations within one second can be achieved as may be desirable for fine control in ventilator applications. This also shows that the valve is appropriate for use in resistance measurements, as the Airflow Perturbation Device has been shown to produce usable measurements at frequencies as low as 7 Hz.

The flow curves of lower frequencies in this graph include an unexpected shoulder during the closing movement as shown in Figure 17 below. The cause of this has not been proven but is thought to be a result of spring interaction with the edge of the recess into which the spring compacts during the closing motion. This catch can be felt when actuating the valve by hand. The 0.532 N/mm springs used during dynamic testing had a diameter 0.04 mm larger than the original 0.039 N/mm springs for which these holes were drilled. This could be corrected by re-drilling but was not done in this case in order to allow the smaller springs to continue to be used in later tests if desired without instability created by lateral motion of the valve quarters. This catch could also be avoided by using the spring guides of the original design, but this was not done because the effect did not appear to be detrimental to the testing done here.

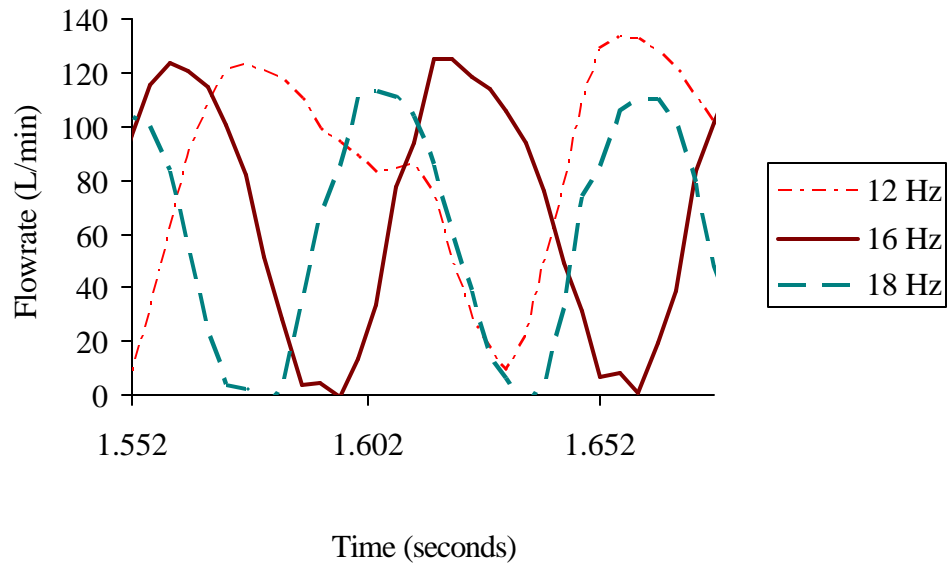


Figure 17: Detailed View of Valve Response to High Frequencies

Finally, resistance measurements were attempted in order to reinforce the conclusion that adequate flow changes are produced by the valve to allow its use in conjunction with the APD. The comparison of results in Figure 18 shows that although the valve-perturbed measurement did not precisely match the wheel-perturbed number for the same conditions, there is a strong, predictable relationship between the two, with a least-squares analysis result of ($R^2 = 0.9843$ for inhalation, $R^2 = 0.9867$ for exhalation). No attempt was made to recalibrate the device for the greater resistance created by adding the valve into the existing flow path, and this certainly accounts for at least a portion of the difference between the two measurements. The APD software could be slightly modified to account for the difference in calibration.

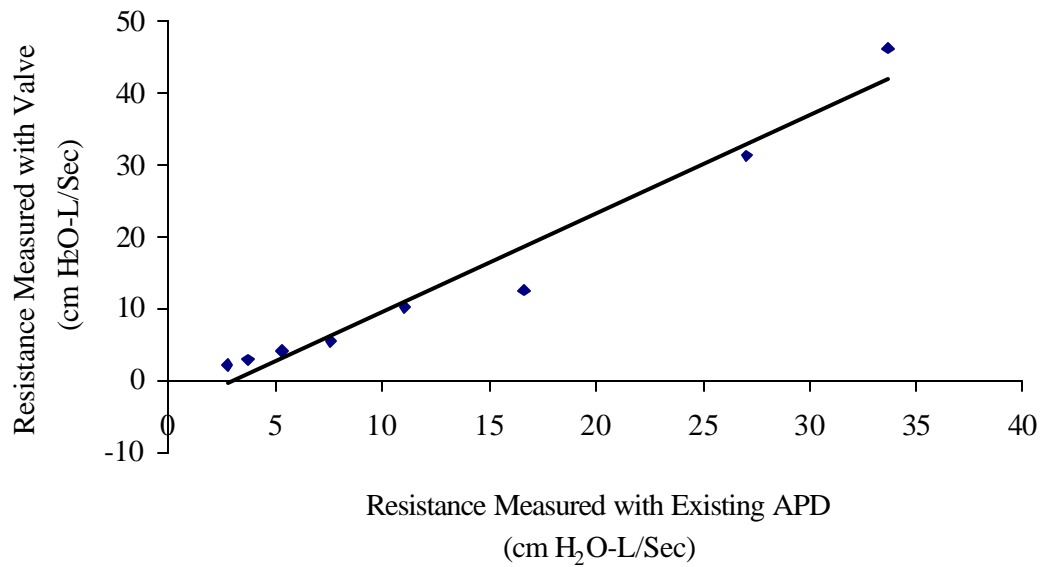
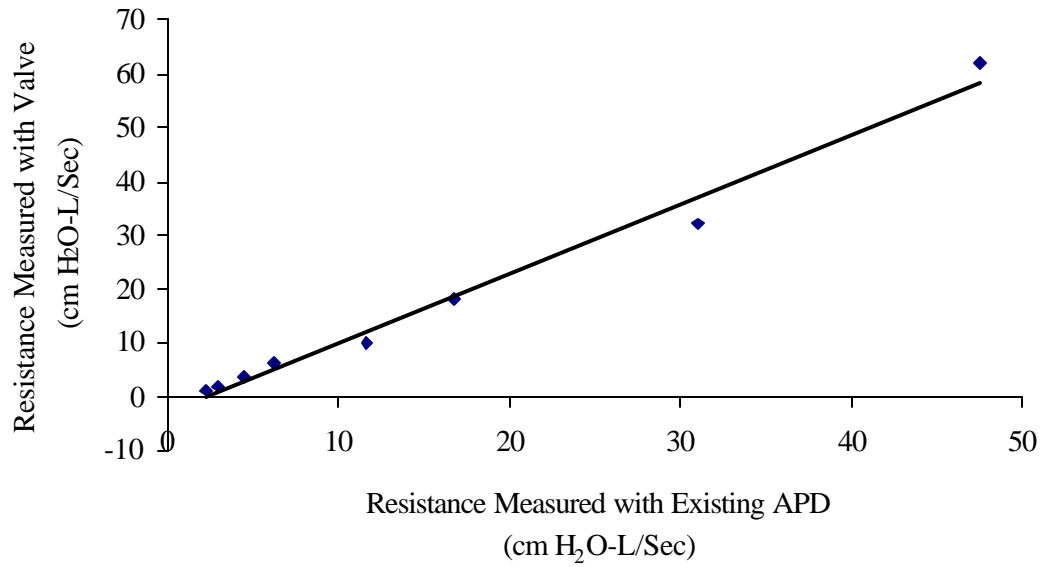


Figure 18: Comparison of Current and Proposed APD Performance – Inhalation (top) and Exhalation (bottom)

The valve as built is a good replacement for the existing air perturbation mechanism. The current slotted disk design is subject to frequent binding, particularly in the high-moisture environment of ventilatory applications. In addition, air flow causes the wheel to slow, particularly in high-flow conditions, which may interfere with the calculation of resistance. The valve is subject to neither of these difficulties. It is robust and steady in its operation. With a slight modification to the current housing design, it could be driven by the electric motor already used in the APD to turn the perturbation wheel.

The current APD is also physically built only for breathing to the open environment and has significant leaks. With the valve housing as built it is a completely sealed, symmetric system and would require no further adaptation to connect it between a mechanical ventilator and a patient, if it is desired to proceed with the cable-driven approach rather than waiting for usable electroactive polymer technology to achieve a workable actuator.

An attempt was made to measure breathing resistances against a downstream capacitance in order to demonstrate this type of application. This could not be completed because the current APD software is designed to measure negative mouth pressures during inhalation, while a positive pressure forcing air into the mouth causes negative pressure to never be achieved. The program therefore returns a null result for resistance. This will be the subject of further development within the APD project.

Chapter 6: Conclusions

The valve designed as part of this work represents a new type of fluid flow control mechanism with a geometry different from that of existing valves. Our design allows the use of circumferential actuation that minimizes actuator travel during valve stroke. Its small mass and resulting low inertia allow the rapid actuation demanded of air-control devices in medical settings. The valve's throttling characteristics are favorable and predictable, with a smooth profile across the range of operation. Furthermore, the new valve is a suitable replacement for the current perturbation mechanism in the Airflow Perturbation Device. Our design is simple and robust in the presence of humidity and high-velocity flows.

6.1 Recommendations for Further Study

It was clear during our experiments that the speed of valve's step response was limited by the speed at which the motor could rotate, not by the design of the valve. The step response experiments and the analysis of valve dynamics point to a much higher operating frequency than the ones generated by the actuator used in our setup.

The mechanical characteristics of the valve can be further improved. The Gore-TEX® cable used to drive the valve tended to bind or fray after an hour or two of motion. This was largely caused by crudely drilling a hole in the housing through which the cable passed. The cable hole was also the source of significant air leakage if not packed carefully. This passage should be redesigned to resolve

both problems, and other low-friction, high-strength cable materials should be considered.

Friction between the moving valve parts and the housing surface normal to flow necessitated the use of fairly stiff springs to ensure that the valve would open, even in the presence of a high differential pressure. The friction between wedges and housing increased in the presence of collected moisture, which would certainly be present in a ventilator application. Consideration should be given to the geometry of this interface.

The head loss caused by the valve in its open state is fairly large, but might be reduced by creating a tapered surface normal to flow rather than the flat plane used in this case. Redesigning the three-dimensional shape of the valve wedges would be a useful focus of improved design.

Finally, the capabilities of this valve make it physically possible to perform rapid closed-loop control of assisted breathing. Software will have to be created for valve control and to adapt the APD to operation in the presence of a mechanical ventilator.

Bibliography

- Abreu, M. Gama. 2001. Monitoring the Pulmonary Function of the Patient with ARDS. Thes. University Clinic Carl Gustav Carus, Dresden University of Technology.
- Aestiva. 2004. Product Brochure for 5 MRI Anesthesia Machine.
- American Thoracic Society, with the European Society of Intensive Care Medicine, and Le Societe de Reanimation de Langue Francaise. 1999. "Internal Consensus Conferences in Intensive Care Medicine: Ventilator-associated Lung Injury in ARDS." Respiratory Critical Care Medicine 160: 2118-2124.
- American Thoracic Society. 1994. "Standardization of Spirometry: 1994 Update." Official Statement of the American Thoracic Society, Adopted by its Board of Directors, 11 November 1994.
- ARDS Network. 2000. "Ventilation with Lower Tidal Volumes as Compared with Traditional Tidal Volumes for Acute Lung Injury and the Acute Respiratory Distress Syndrome." The New England Journal of Medicine 342(18): 1301-1308.
- Aslanian, Pierre, Souhail El Atrous, Daniel Isabey, Elisabeth Valente, Daniella Corsi, Alain Harf, Francois Lemaire, and Laurent Brochard. 1998. "Effects of Flow Triggering on Breathing Effort During Partial Ventilatory Support." American Journal of Respiratory Critical Care Medicine 157: 135-143.
- Aveox. 2004. Medical Motor Type 1005 Product Specifications.
- Brunner, J. X. 2002. "History and Principles of Closed-loop Control Applied to Mechanical Ventilation." Nederlandse Vereniging voor Intensive Care 6(4): 6-9.
- Catlin, Elizabeth A. 1998. "Mechanical Ventilation in the Neonate." Internal memorandum from the Harvard and Massachusetts General Hospital Departemnt of Neonatology.
- Chao, David, David J. Scheinhorn, and Meg Stearn-Hassenpflug. 1997. "Patient-ventilator Trigger Asynchrony in Prolonged Mechanical Ventilation." Clinical Investigations in Critical Care 112(6): 1592-1599.
- Conti, Georgio, Massimo Antonelli, Silvia Arzano, and Alessandro Gasparetto. 1997. "Equipment Review: Measurement of Occlusion Pressures in Critically Ill Patients." Critical Care 1(3): 89-93.

- Du, Hong-Lin, Mikiya Ohtsuji, Masaki Shigeta, David C. Chao, Katsunori Sasaki, Yutaka Usuda, and Yoshitsugu Yamada. 2001. "Expiratory Asynchrony in Proportional Assist Ventilation." American Journal of Respiratory Critical Care Medicine 165: 972-977.
- Emerson. 2003. Personal communication.
- Esteban, Andres, Fernando Frutos, Martin Tobin, Inmaculada Alia, Jose Solsona, Inmaculada Valverde, Rafael Fernandez, Miguel A. De La Cal, Salvador Benito, Roser Tomas, Demetrio Carriedo, Santiago Macias, and Jesus Blanco. 1995. "A Comparison of Four Methods of Weaning Patients from Mechanical Ventilation." The New England Journal of Medicine 332(6): 345-350.
- Farré, Ramon, Marco Mancini, Mar Rotger, Miquel Ferrer, Josep Roca, and Daniel Navajas. 2001. "Oscillatory Resistance Measured during Noninvasive Proportional Assist Ventilation." American Journal of Respiratory Critical Care Medicine. 164: 790-794.
- Field, Karen A.. 2003. "Engineers Fight SARS." Design News 4 August 2003.
- Gawande, Atul. 2002. Complications. New York: Picador USA.
- Gomella, Leonard G. 1998. Clinician's Pocket Reference. 7th ed. Norwalk, Connecticut: Appleton and Lange.
- Grasso, Salvatore, Filomena Puntillo, Luciana Mascia, Giovanni Ancona, Tommaso Fiore, Francesco Bruno, Arthur Slutsky, and V. Marco Ranieri. 2000. "Compensation for Increase in Respiratory Workload during Mechanical Ventilation." American Journal of Respiratory Critical Care Medicine 161:819-826.
- Holland, W. P., A. F. Verbraak, J. M. Bogaard, and W. Boender. 1986. "Effective Airway Resistance: A Reliable Variable from Body Plethysmography." Clinical Physiology and Physiology Measurement 7(4): 319-331.
- Hubmayr, Rolf D., Martin D. Abel, and Kai Rehder. 1990. "Physiologic Approach to Mechanical Ventilation." Critical Care Medicine 18(1): 103-113.
- Johnson, A. T., H. M. Berlin, and S. A. Purnell. 1974. "Perturbation Device for Noninvasive Measurement of Airways Resistance." Medical Instrumentation 8:141.
- Johnson, Arthur T. 1991. Biomechanics and Exercise Physiology. New York: John Wiley and Sons, Inc.

- Kosarzecki, Connie. 2003. "Proportional Flow Controls." Command Controls Corporation Product Brochure.
- Kreit, J. W., M. W. Capper, and W. L. Eschenbacher. 1994. "Patient Work of Breathing During Pressure Support and Volume-cycled Mechanical Ventilation." American Journal of Respiratory Critical Care Medicine 149(5): 1085-1091.
- Lausted, Christopher G., and Arthur T. Johnson. 1999. "Respiratory Resistance Measured by an Airflow Perturbation Device." Physiological Measurement 20: 21-35.
- Martini, Frederic. Fundamentals of Anatomy and Physiology. Upper Saddle River, New Jersey: Prentice Hall.
- Matthay, Frank J. A. 2003. "Science Review: Mechanisms of Ventilator-Induced Injury." Critical Care 7(3): 233-41.
- Munson, Bruce R., Donald F. Young, and Theodore H. Okiishi. 1994. Fundamentals of Fluid Mechanics. 2nd ed. New York: John Wiley and Sons, Inc.
- Navajas, Daniel and Ramon Farre. 2001. "Forced Oscillation Assessment of Respiratory Mechanics in Ventilated Patients." Critical Care Medicine 5(1): 3-9.
- Phipps and Bird, Internal memorandum. Pneumotachographe De Fleisch, Modèle n.3. April, 2004.
- Puritan Bennet. 2003. Personal communication.
- Puritan Bennet. 2003. Product Brochure on Achieva Model Ventilator.
- Ranieri, V. Marco, Rocco Giuliani, Luciana Mascia, Salvatore Grasso, Vito Petruzzelli, Muccia Puntillo, Gaetano Perchiazzi, Tommaso Fiore, and Antonia Brienza. 1996. "Patient-ventilator Interaction During Acute Hypercapnia: Pressure-support vs. Proportional-Assist Ventilation." The American Physiological Society 161: 426-436.
- Sahota, Manjit Singh. 1998. Validation of the Airflow Perturbation Device and the Pressure Flow Characteristics of Excised Sheep Lungs. Diss. University of Maryland.
- SensorMedics. 2003. Personal communication.
- Tobin, Martin, Amal Jubran, and Franco Laghi. 2001. "Patient-Ventilator Interaction." American Journal of Respiratory and Critical Care Medicine 163(5): 1059-1072.

- Tobin, Martin. 2001. "Ventilator Monitoring, and Sharing the Data with Patients." American Journal of Respiratory and Critical Care Medicine 163: 810-811.
- Vo, Quang Viet. 1987. The Airflow Perturbation Device Ventilated. Thes. University of Maryland.
- Walls, Ron, Robert Luten, Michael Murphy, and Robert Schneider. 1997. Manual of Emergency Airway Management. Philadelphia: Lippincott Williams & Wilkins Publishers.
- Whitehead, T. and A. S. Slutsky. 2002. "The Pulmonary Physician in Critical Care – 7: Ventilator Induced Lung Injury." Thorax 57: 635-642.
- Yamada, Yoshitsugu, and Hong-Lin Du. 2000. "Analysis of the Mechanisms of Expiratory Asynchrony in Pressure Support Ventilation: A Mathematical Approach." Journal of Applied Physiology 88(6): 2143-2158.
- Yang, Karl L., and Martin Tobin. 1991. "A Prospective Study of Indexes Predicting the Outcome of Trials of Weaning from Mechanical Ventilation." The New England Journal of Medicine 324(21): 1445-1450.